The International Journal of Advanced Manufacturing Technology
https://doi.org/10.1007/s00170-025-16382-1

ORIGINAL ARTICLE

# Defect detection in 3D printing: a review of image processing and machine vision techniques

**Elham Armin[1] · Saleh Ebrahimian[1] · Mehdi Sanjari[1] · Peyman Saidi[2] · Hamid-Reza Pourreza[3]**

Received: 26 April 2025 / Accepted: 11 August 2025


**Abstract**
Detecting defects in 3D printing has become crucial as additive manufacturing gains traction in key industries like aerospace, automotive, and healthcare. This paper offers a thorough review of the methods used for defect detection in 3D printing, highlighting image processing, machine vision, and the integration of deep learning techniques. It contrasts traditional methods, which depend on manual feature extraction and classification algorithms, with modern deep learning approaches that automate feature extraction and classification in a unified process. Additionally, the paper compares full-reference methods—where defects are detected by comparing printed parts against ideal reference models—with no-reference methods that identify anomalies without predefined models. The review also explores real-time monitoring systems that allow for early defect detection during printing, reducing production failures and material waste. Future developments are anticipated to focus on autonomous feedback mechanisms, fostering innovation in defect prevention and improving the sustainability of 3D printing processes.

**Keywords** Anomaly detection · Image processing · Machine vision · Deep learning · Additive manufacturing

## 1 Introduction

Defect detection in 3D[1] printing has become a critical area of research, particularly as additive manufacturing (AM) technologies are increasingly used in high-stakes industries such as aerospace, automotive, and healthcare [1, 2]. While 3D printing offers unique advantages in producing complex geometries and custom parts, the process is prone to various defects that can compromise the structural integrity, dimensional accuracy, and surface finish of the printed objects [3–7]. These defects, if undetected, may lead to significant material waste, increased production costs, and failures in functional components. As such, real-time defect detection has emerged as an essential tool for ensuring the quality and reliability of 3D-printed parts [8].

3D printing, also known as additive manufacturing, is a process that builds objects layer by layer from digital models. Among the commonly used 3D printing technologies are fused deposition modeling (FDM), stereolithography (SLA), selective laser sintering (SLS), and direct metal laser sintering (DMLS). Each technology comes with its own set of advantages and limitations, but all are susceptible to defects that can impact the final product.

For example, in FDM, defects such as layer misalignment, stringing, and under-extrusion are common due to the extrusion process's inherent limitations and environmental factors like uneven cooling [9]. Similarly, porosity and surface roughness are typical issues in SLS and DMLS, where incomplete sintering of the powder can lead to poor layer bonding and reduced mechanical strength [10]. These defects necessitate the development of advanced monitoring systems to detect issues as they arise and prevent defective parts from being produced.

As 3D printing technologies evolve, there is an increasing demand for reliable, automated defect detection systems. Traditional post-production inspection methods, such as manual, X-ray, or ultrasonic scanning, are costly, time consuming, and impractical for use in real time. Moreover, these methods detect defects only after the part has been fully printed, making it impossible to correct errors during

✉ Hamid-Reza Pourreza
hpourreza@um.ac.ir

1 AI-Innovate Solutions Inc, Oakville, ON, Canada

2 Queen's University, Kingston, ON, Canada

3 Ferdowsi University of Mashhad, Mashhad, Iran

[1] Three-dimensional.

Published online: 29 August 2025

the process and resulting in material waste and production delays [11].

Real-time defect detection, on the other hand, can identify and address defects as they occur, ensuring that errors are corrected during the printing process itself. This capability is particularly important for industries where part failure can have serious consequences, such as in aerospace or medical applications. By minimizing waste and improving the reliability of printed components, real-time defect detection plays a critical role in enhancing the efficiency and sustainability of 3D printing [12, 13].

Image processing and machine vision technologies offer promising solutions to the challenges of real-time defect detection in 3D printing [1, 3, 14–19]. These technologies utilize cameras and image analysis algorithms to continuously monitor the printing process and detect anomalies such as surface roughness, layer misalignment, and incomplete deposition. By employing techniques like edge detection, texture analysis, and feature extraction, image processing systems can identify defects in real time, triggering corrective actions before the defect affects the entire part [20].

In recent years, machine learning and deep learning have also been integrated into defect detection systems, enabling more accurate and predictive monitoring. Machine learning models can be trained on large datasets of 3D-printed parts with known defects, allowing them to automatically classify and detect issues during the printing process. This combination of traditional image processing techniques with machine learning models offers a powerful approach to ensuring the quality and reliability of 3D-printed parts [21].

While limited studies have explored defect detection in additive manufacturing, our paper offers a distinct contribution by providing a comprehensive review of both classical and modern image processing techniques in defect detection, integrating recent advancements in deep learning. A closely related study by Kim et al. [22] provides an extensive survey of image-based fault monitoring, emphasizing machine learning algorithms and vision-based methods for detecting anomalies in AM processes. Their work focuses on the application of sensor-driven monitoring systems and deep learning models to classify defects using image data. However, our review expands upon this by incorporating a comparative analysis of full-reference and no-reference approaches, evaluating their effectiveness across different 3D printing technologies. Additionally, our study provides a structured comparison of defect detection methodologies, categorizing them based on their computational complexity, adaptability, and real-time applicability. By highlighting the strengths and limitations of both classical and AI-driven defect detection systems, our work serves as a foundation for future research in hybrid AI-enhanced monitoring systems that integrate image processing with adaptive feedback mechanisms for real-time quality control in 3D printing.

In the remainder of this paper, Sect. 2 will provide an overview of various 3D printing technologies while also introducing the defects that may arise during the printing process. Given the importance of detecting these defects in real time, which can not only reduce material waste but also lower production time and costs, the latter part of Sect. 2 will explore various defect detection methods based on visual inspection. Next, Sect. 3 will offer a more detailed discussion of classical and modern defect detection techniques, highlighting their similarities and differences. Sections 4 and 5 will then present published research related to these two categories of techniques. The classification of defect detection methods into no-reference and full-reference approaches has also been considered in distinguishing between these two categories. Following this, Sect. 6 will compare different detection algorithms. Since defect detection can serve as a real-time feedback mechanism in 3D printers, allowing the printer to attempt defect correction, Sect. 7 will introduce real-time feedback systems. Finally, Sect. 8 will provide a conclusion and discuss future directions in the field.

## 2 Background

As additive manufacturing (AM) becomes integral to high-precision industries such as aerospace, biomedical engineering, and automotive production, ensuring defect-free fabrication is paramount. Even minor defects can compromise structural integrity, mechanical performance, and aesthetic quality, necessitating robust defect detection methodologies. These methodologies leverage advanced computational techniques, including image processing, machine vision, and deep learning, to enhance quality control and optimize manufacturing efficiency.

The overarching goal of defect detection is to enable real-time identification and correction of anomalies, thereby reducing material waste, minimizing production costs, and enhancing the reliability of printed components. Significant advancements in sensor technology, artificial intelligence, and data analytics have paved the way for automated and highly accurate defect detection mechanisms. This section provides a comprehensive examination of the foundational technologies of 3D printing, common defect typologies, and the evolution of state-of-the-art defect detection methodologies.

### 2.1 Classification of 3D printing technologies

AM technologies are broadly categorized based on either the material used, polymer-based and metal-based systems, or the underlying printing mechanism, light-induced and nozzle-based methods.

- Polymer-based AM utilizes thermoplastic filaments, photopolymer resins, or polymer powders. Common techniques include fused deposition modeling (FDM), stereolithography (SLA), digital light processing (DLP), and selective laser sintering (SLS). These methods are widely used for prototyping and producing lightweight components.
- Metal-based AM fabricates metal parts using powder or wire feedstock and high-energy sources. Key technologies include laser powder bed fusion (LPBF), directed energy deposition (DED), wire arc additive manufacturing (WAAM), additive friction stir deposition (AFSD), and cold spray. These processes are essential for high-performance applications in aerospace, defense, and industrial manufacturing.

A second, equally important classification is based on the fabrication mechanism, which organizes processes into two main groups: light-induced methods and nozzle-based methods. This classification is particularly relevant for understanding common defects.

#### 2.1.1 Light-induced methods

These processes use a focused light source (e.g., a laser or digital projector) to selectively fuse or cure material in a layer-by-layer fashion. This category includes both polymer- and metal-based techniques.

- Stereolithography (SLA): A UV laser cures a photopolymer resin, producing high-resolution parts with a smooth surface finish. Common defects include over-curing, under-curing, and layer detachment [12].
- Digital light processing (DLP): Like SLA, DLP uses a digital projector for faster curing. Typical issues are voxel distortion and uneven curing.
- Laser powder bed fusion (LPBF): This process, which includes selective laser melting (SLM), employs a high-powered laser to fully melt and fuse metal powders. Defects such as keyhole porosity, lack of fusion, and residual thermal stress are common due to high thermal gradients [10] [11]. Selective laser sintering (SLS) is a related process for polymers that uses a laser to partially sinter powdered material, which can lead to surface roughness and porosity.
- Continuous liquid interface production (CLIP): An advanced form of photopolymerization, CLIP improves mechanical properties and reduces visible layer lines. Limitations include resin instability and oxygen diffusion inconsistencies.

#### 2.1.2 Nozzle-based methods

These methods build objects by extruding or depositing material through a nozzle. The category includes both polymer-based extrusion and high-temperature deposition for metals.

- Fused deposition modeling (FDM): Also known as fused filament fabrication (FFF), this method melts and deposits its thermoplastic filament layer by layer. Typical defects include warping, layer misalignment, and under-extrusion [9].
- Direct ink writing (DIW): Also referred to as robocasting, this process deposits pastes or gels through fine nozzles. Common issues are flow inconsistencies and air entrapment.
- Directed energy deposition (DED): Also known as laser metal deposition (LMD), this process injects powder or wire into a melt pool created by a laser or electron beam. Defects often include surface roughness, un-melted particles, and low dimensional precision.
- Wire arc additive manufacturing (WAAM): An electric arc melts metal wire to deposit layers. While cost-effective for large parts, WAAM is prone to high residual stresses and dimensional inaccuracies that require post-processing.
- Additive friction stir deposition (AFSD): A solid-state process where a rotating tool plastically deforms and deposits material. Defects may include void formation, irregular material flow, and a lack of bonding in complex geometries.
- Cold spray: This solid-state process accelerates metal particles to supersonic speeds for deposition without melting. This method avoids thermal distortion, though it can still be affected by porosity and weak bonding.

### 2.2 Common defects in 3D printing

The output quality of additive manufacturing is influenced by several critical parameters, including layer thickness, printing speed, extrusion temperature, and material properties. A thorough understanding of the AM process, encompassing material characteristics and the interplay of process-structure-properties, is essential to ensuring high product quality. Identifying and addressing defects early in the fabrication process is crucial to mitigating faults and improving the reliability of printed parts. Defects in AM can be categorized based on their impact on geometry and dimensions, surface quality, microstructure, or mechanical properties. The most common defects include the following:

**Geometrical inaccuracy:** Geometrical inaccuracy refers to the deviation of a printed object's shape or dimensions from its intended design. This defect arises due to factors such as improper bed leveling, insufficient cooling, or residual stress accumulation. Advanced in situ monitoring techniques, such as structured light scanning and digital image correlation, enable early detection and correction of dimensional deviations.

**Layer misalignment:** This defect occurs when successive layers are misaligned during printing, usually due to mechanical errors such as poor calibration or external vibrations. Layer misalignment can compromise both the structural integrity and aesthetic quality of the printed object. For instance, in FDM printing, this defect is a leading cause of weak inter-layer bonding, which can result in part failure under load [9] (Fig. 1a).

**Porosity:** Porosity refers to voids or air pockets within the printed object. In powder-based processes like SLS and DMLS, incomplete fusion of powder particles often results in porous structures. Porosity significantly weakens the part's mechanical properties, making it more prone to failure under stress. Detection of porosity during printing is essential to ensure the durability of the final product [10] (Fig. 1b).

**Surface roughness and texture defects:** Surface roughness and inconsistencies in texture are common across various 3D printing methods, often resulting from incomplete layer bonding or improper curing. Although surface defects primarily affect the aesthetic quality of the part, they can also lead to mechanical issues, especially in parts requiring high precision. Detecting and correcting surface roughness is important for ensuring part performance [8] (Fig. 1c).

**Warping:** Warping occurs when parts cool unevenly during the printing process, causing the edges or corners to deform. This defect is particularly common in FDM and SLA processes due to thermal expansion and contraction of the material. Warping can lead to dimensional inaccuracies, preventing the part from meeting design specifications. Early detection of warping can prevent apart from becoming unusable, reducing material wastage [20] (Fig. 1d).

**Incomplete layer deposition:** Incomplete layer deposition occurs when insufficient material is extruded or

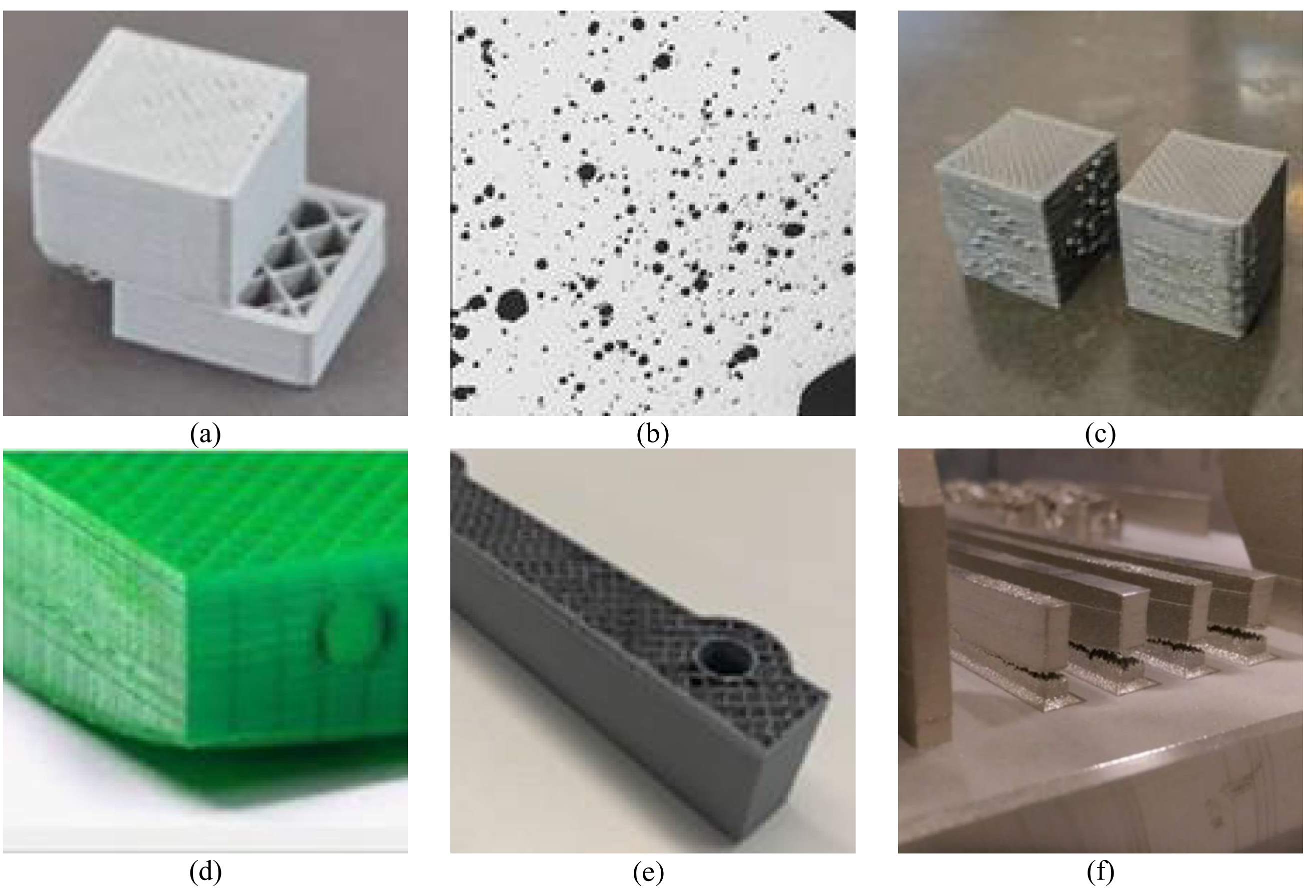


**Fig. 1** The most common types of defects encountered in 3D printing: (a) layer misalignment, (b) porosity, (https://3dincredible.com/the-rising-concern-of-porosity-in-metal-3d-printing-materials/.) (c) surface roughness and texture defects, (d) warping, (e) incomplete layer deposition, (f) cracking and residual stress (https://3dprintingindustry.com/news/zurich-researchers-simulate-residual-deformations-in-slm-3d-printed-parts-172408/.)

deposited, resulting in thin layers or gaps. This can be caused by clogged nozzles, under-extrusion, or incorrect printing parameters. This defect weakens the part, leading to structural deficiencies. In applications requiring load-bearing components, early detection of under-extrusion is critical to ensuring part viability [23] (Fig. 1e).

**Cracking and residual stress:** Cracking occurs in high-temperature processes like DMLS due to residual stresses that build up as the material cools unevenly. If the internal stresses exceed the material's yield strength, cracks may form, compromising the part's integrity. Cracks are particularly dangerous in metal components intended for high-stress environments. Detecting such defects in real time allows for adjustments to printing parameters that can mitigate thermal stress [11] (Fig. 1f).

Based on the idea presented by Kim et al. [22], Fig. 2 classifies typical defect types in AM based on their impact domains, such as geometry, surface quality, microstructure, and mechanical performance. It is important to distinguish that defects like porosity, delamination, and cracking are not mechanical properties themselves, but rather they adversely affect mechanical properties such as strength, ductility, or fatigue life.

Another important source of defects, particularly in metal-based additive manufacturing processes, is the reheating effect that occurs during multi-layer printing. As new layers are deposited, the underlying material experiences repeated thermal cycling, which can lead to the remelting and re-solidification of previously solidified regions. This reheating may induce the formation of new pores due to molten material flow and gas entrapment. Additionally, repeated heating promotes abnormal grain growth and recrystallization, which can deteriorate the microstructure and reduce mechanical performance. It may also lead to the redistribution or accumulation of residual stress across the build, increasing the risk of warping, delamination, or cracking in subsequent layers. Understanding and mitigating the impact of thermal history is critical for improving the reliability of multi-layer printed components.

### 2.3 Evolution of defect detection methodologies

Defect detection has progressed from manual post-processing inspections to real-time automated monitoring systems. Advanced computational approaches have revolutionized defect identification, enabling proactive quality control.

#### 2.3.1 Manual inspection and traditional methods

Historically, defect detection relied on human inspection, X-ray imaging, and ultrasonic testing. While effective, these approaches were time intensive and unsuitable for real-time process control.

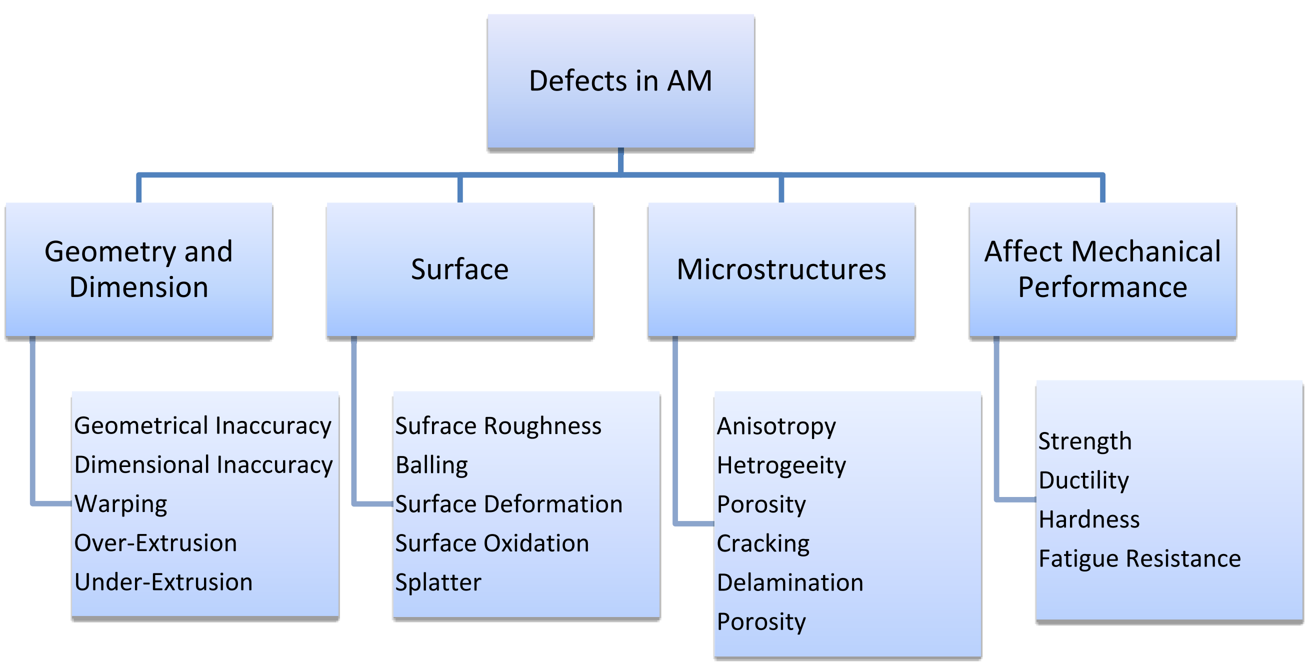


**Fig. 2** Classification of common additive manufacturing defects based on the aspect of the printed part they affect. Note: Defects such as porosity, cracking, and delamination are not mechanical properties themselves but contribute to the degradation of mechanical performance metrics like strength or ductility

### 2.3.2 Automated inspection

Automated inspection techniques have become essential in modern additive manufacturing (AM) for ensuring high-quality output and reducing material waste. Among various automatic inspection techniques, *visual inspection* remains one of the most critical due to its ability to rapidly detect surface-level defects in real time. Automated visual inspection systems leverage high-resolution imaging, computer vision algorithms, and artificial intelligence to analyze and classify surface anomalies. These systems can detect catastrophic defects such as layer misalignment, incomplete, and spaghetti easily.

A visual inspection system for defect detection comprises an imaging module, which includes a camera and an illumination system. The camera operates in either the visible or infrared spectrum. Visible-spectrum cameras are typically used for capturing high-resolution 2D images of printed surfaces, while infrared (thermal) cameras are increasingly employed to monitor the heat distribution and detect anomalies such as overheating, under-sintering, or thermal delamination [24]. The use of thermographic imaging not only helps to detect surface defects but can also be used to identify subsurface defects [25]. Thermal cameras, however, require careful calibration to ensure accurate temperature measurements. For this purpose, thermocouples are frequently used as ground-truth temperature references during setup and process validation [26]. Although thermocouples provide only one-dimensional (1D) data, their readings are essential for validating thermal models and calibrating infrared imaging systems. In some hybrid monitoring systems, thermocouple data is also used in real time to detect abnormal thermal events and inform corrective actions during the build process.

In addition to 2D and thermal imaging, 3D reconstruction techniques are also employed—particularly for post-print inspection—where a complete point cloud of the final object is generated using structured light scanners or laser-based 3D scanners. These techniques allow for a full geometric comparison with the original CAD model, enabling the detection of dimensional deviations, warping, or surface anomalies that may not be apparent in 2D images.

For in situ inspection during the printing process, it is crucial to synchronize image acquisition with the active printing layer or movement defined in the G-code. To enable this synchronization, modifications are often made to the G-code to insert camera trigger commands or metadata tags at predefined intervals [4, 5]. This approach ensures that each captured image corresponds to a specific layer or print event, facilitating accurate layer-wise defect detection and process analysis.

Captured images are analyzed using traditional or advanced image processing and machine vision techniques to identify defects. Upon defect detection, the system may either halt the printing process or initiate corrective actions to address the issue.

Early vision-based automated defect detection systems relied on classic computer vision techniques [27]. These conventional approaches extracted mid-level features such as edges, textures, and contours using handcrafted methods. Defect identification was then performed using simple decision-making algorithms. While computationally efficient, these methods struggled with complex geometries and variations in the manufacturing process.

To enhance detection accuracy, machine learning algorithms were later integrated to classify these manually extracted features. While machine learning improved pattern recognition and defect classification [28], the reliance on manual feature engineering remained a limitation, reducing adaptability to varying defect types.

In contrast, modern deep learning–based models have revolutionized defect detection by eliminating the need for manual feature extraction. These models achieve unprecedented precision by learning feature representationsand classification directly from raw data, enabling more robust and adaptive defect detection [28].

We will explain these methods in more detail below.

To provide a structured understanding of defect detection methodologies, Fig. 3 and Table 1 present a hierarchical classification of defect detection strategies, spanning classic inspection methods to state-of-the-art AI-driven solutions.

It should be noted that most defect detection methods have attempted to detect the defect while printing. In other words, they are based on real-time implementation. Imaging and execution of the defect detection algorithm are generally performed layer by layer or, for every few layers, printed. The low printing speed causes the time interval between two consecutive images to be so long that it does not pose a major concern for the implementation of the algorithms in real time. The variety of computational load in different techniques (Table 1) allows for the selection of a suitable algorithm for real-time detection, depending on the available processing infrastructure.

As AM continues to evolve, the need for high-fidelity defect detection is more pressing than ever. The transition from manual inspections to AI-powered real-time monitoring has significantly improved defect identification and resolution. Future research should focus on hybrid AI systems, integrating multimodal sensor data, and adaptive machine learning models to further enhance defect detection capabilities in AM.

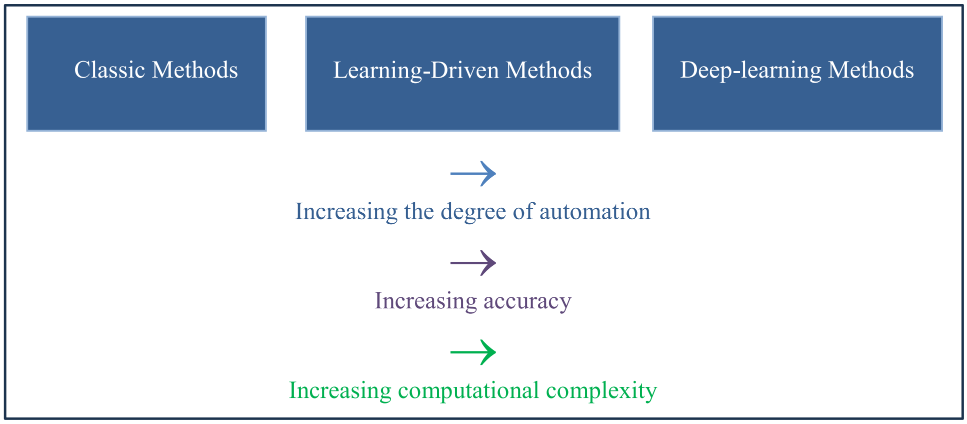


**Fig. 3** Comparison of defect detection strategies

**Table 1** Key features of defect detection strategies

| Approach | Feature extraction | Classification | Accuracy | Computational complexity | Advantages | Limitations |
|---|---|---|---|---|---|---|
| Classical approaches | Manual (edge detection, thresholding) | Manual | Moderate | Low | Fast, computationally efficient | Limited robustness, struggles with complex geometries |
| Learning-driven approaches | Manual feature engineering (SVM, Random Forest, KNN) | Automated | High | Moderate | Improved accuracy over classical methods | Requires labeled data, feature engineering effort |
| Deep learning approaches | Automated feature extraction (CNNs, Autoencoders, Transformers) | Automated | Very High | High | Fully automated, highly accurate | Requires large datasets and computational resources |

## 3 Defect detection: classic and modern algorithms

Defect detection is basically a pattern classification problem. Pattern classification is a fundamental process in machine learning and computer vision, aimed at assigning input data to predefined categories or classes based on identifiable patterns. A pattern classification system typically consists of two main components: *feature extraction* and *feature classification* [29, 30].

**Feature extraction**: This is the process of identifying and selecting the most relevant features from raw data that best represent the underlying patterns. In image processing, for example, features could be edges, textures, shapes, or colors. The goal of feature extraction is to reduce the complexity of the data while preserving the important information necessary for distinguishing between different classes.

**Feature classification**: Once features are extracted, the classification component uses these features to assign the data to a specific category. This step involves applying classification algorithms to decide which class the input data belongs to, based on the extracted feature set.

Pattern recognition methods can be classified into two categories based on how the feature vector is generated. The first category involves manually creating the feature vector, often referred to as classical methods. In contrast, modern methods rely on the feature vector being derived through a learning process. The following sub-sections will provide a short description and comparison of these two approaches.

### 3.1 Classical approach to pattern classification

In traditional pattern classification systems, these two stages, feature extraction and classification, are handled separately. Feature extraction was usually performed using handcrafted methods, where domain experts manually designed algorithms to extract specific features that are known to be useful. For example, in image processing, techniques like edge detection (e.g., Sobel or Canny filters) or texture analysis (e.g., Gabor filters) were often used [27, 28].

For classification, classical algorithms such as Support Vector Machines (SVMs), k-Nearest Neighbors (k-NN), and Decision Trees were applied to the extracted features. These models relied on a predefined set of rules or functions to classify the input data based on the identified patterns. While effective in many applications, this approach had limitations, especially when dealing with complex, high-dimensional data, as the performance heavily depended on the quality of the hand-engineered features [28, 29].

### 3.2 Modern, deep learning–based approach

In contrast, modern approaches to pattern classification, especially in deep learning, integrate feature extraction and classification into a single, learning-based system. This has been made possible by advancements in neural networks, particularly Convolutional Neural Networks (CNNs) for image-based tasks. In these systems, the network automatically learns the best features from the data during training, eliminating the need for manually designed feature extractors [31].

In deep learning models, feature extraction is performed in the early layers of the network, where the model learns to detect low-level features like edges or textures. As the data passes through deeper layers, the network learns more abstract and high-level features, such as shapes and object parts. The classification is handled in the final layers, where the network uses the learned features to classify the input data into specific categories. This approach not only simplifies the design process but also significantly improves performance, particularly in tasks involving complex data, such as image [31].

The integration of feature extraction and classification into a single, end-to-end learning system has made modern pattern classification more powerful and scalable. These systems excel in handling large amounts of data and can automatically learn from it without the need for domain-specific knowledge. This paradigm shift has led to significant advancements in fields like image recognition, speech processing, and defect detection in manufacturing [32].

*Defect detection* is a specialized case of pattern classification that focuses on identifying anomalies or defects in products, processes, or materials. In this context, the task is to classify data into “defective” or “non-defective” categories by detecting patterns that deviate from normal behavior. This challenge is heightened by the fact that defects can manifest in various subtle and irregular ways, such as surface imperfections, cracks, or dimensional inaccuracies. For example, in additive manufacturing, defect detection systems often employ machine vision and image processing to identify flaws in 3D-printed parts by recognizing anomalous patterns in layer deposition or surface texture [20]. As a form of pattern classification, defect detection requires effective feature extraction and robust classification models to ensure high accuracy, especially in real-time applications where early detection is critical for minimizing waste and ensuring product quality [8].

## 4 Classic techniques for defect detection

Several papers have been presented on defect detection in 3D printing using classical methods, which can be categorized into two groups. The first group includes methods that utilize reference information for defect detection, referred to here as full-reference methods. In contrast, the second group consists of methods that perform defect detection without using any reference, which will be referred to as no-reference methods.

In the following, the description of the methods presented in these two categories will be discussed.

### 4.1 Classical full-reference methods

In full-reference methods, sensor data collected during the printing process is compared to an ideal reference to identify defects. This discussion focuses on image sensors, which capture either two-dimensional or three-dimensional data, and evaluate either layer by layer during printing or only at the final stage. This data can include visual aspects of the printed part, such as appearance, dimensions, and the movement path of the print head. Reference data can be prepared using CAD[2] design files or images from prior prints. Below, we present articles in this category, arranged chronologically to showcase the progression of these algorithms.

Cheng and Jafari [33] used a camera-based system for real-time monitoring of 3D printing processes, capturing video frames of printed objects. They employed a thresholding algorithm to segment images into binary forms, distinguishing the object from the background. The system identifies errors like object detachment from the print bed and missing material flow by analyzing the movement and continuity of the printed layers. Optical markers are used for camera calibration, and blob detection techniques track objects and detect deviations. The system achieved a detection rate of 60–80% for identified failures, showing potential for reducing material waste and enhancing 3D printing efficiency through early error detection (printing type: nozzle-based).

Straub [9] developed an image processing method to detect defects in 3D-printed objects by capturing images from multiple angles during printing and comparing them with a reference model. Differences are computed at the pixel level based on brightness values, with a scaling factor to determine the significance of discrepancies, flagging these as defects. This method can identify issues like incomplete prints or filament misplacement, allowing early detection of failures (printing type: nozzle-based).

[2] Computer-aided design.

Hurd et al. [34] proposed a quality assurance algorithm that relies on capturing images of selected print layers using a mobile device mounted above the printer bed. These images are compared with 2D reference images generated from the original 3D model to identify discrepancies. The system uses two main methods: image subtraction and image searching. In the image subtraction method, the difference between two consecutive images highlights newly printed areas. The searching algorithm compares captured images directly to the expected layout, identifying deviations. If errors exceed a predefined threshold, the print is paused, and user feedback is requested to either resume or stop the process. This approach ensures cost-effective quality assurance by enabling error detection mid-print, saving time and materials (printing type: nozzle-based).

Ceruti et al. [35] designed a real-time monitoring system using augmented reality (AR) to compare real-time images of printed objects with a virtual reference model. Image processing detects deviations between printed layers and the expected model, enabling operators to intervene and stop printing if necessary. This AR-based system enhances defect detection during additive manufacturing (printing type: nozzle-based).

Johnson et al. [36] proposed an inspection algorithm where inspections are triggered at predefined intervals during printing, and each printed layer's data is analyzed against set tolerances. When deviations from the reference are detected, the system identifies potential defects and notifies the operator. The algorithm allows flexibility in inspection frequency based on part complexity, ensuring timely flaw detection without unnecessary print interruptions (printing type: nozzle-based).

Nuchitprasitchai et al. [37] utilized optical monitoring to compare finished printed parts with reference models (STL files), using a single-camera setup for 2D shape comparison and a two-camera setup for 3D reconstruction. If errors exceed a 5% threshold, the system halts the print for user intervention. This low-cost approach supports various geometries and filament colors (printing type: nozzle-based).

Straub [38] also leveraged visible light imaging to detect both macro- and micro-defects in 3D-printed objects. By capturing multiple images from different perspectives, discrepancies in size, orientation, and fill levels are compared against a reference model. This method ensures the detection of visible and micro-defects, enhancing the reliability of printed products, especially for safety–critical applications (printing type: nozzle-based).

Holzmond and Li [12] proposed an algorithm using 3D digital image correlation (3D-DIC) to capture the geometry of each printed layer and compare it with the corresponding CAD model. Point clouds from the CAD model and 3D-DIC data are aligned using the iterative closest point (ICP) algorithm, calculating $Z$-axis deviations to detect defects like blobs or holes without halting the print (printing type: nozzle-based).

Lyngby et al. [39] developed an algorithm employing a calibrated camera system to capture images after each layer is deposited. These images are segmented and compared with expected segmentation masks from the CAD model, using logical exclusive disjunction to identify issues such as warping and extrusion failure (printing type: nozzle-based).

Delli and Chang [40] integrated image processing with supervised machine learning for real-time 3D printing monitoring. The system captures images at checkpoints, analyzes them using pixel-based RGB[3] analysis, and classifies parts as "good" or "defective" using an SVM. The system halts printing if defects are detected, reducing material and time waste (printing type: nozzle-based).

Malik et al. [41] proposed an algorithm that captures top-view images of each layer during the 3D printing process, reconstructing a 3D model in real time. It processes these images using MATLAB, aligning them with the layer information extracted from the G-code. This alignment ensures accurate layer identification and enables detailed inspection of both surface and internal structures. Defects can be detected layer by layer through this model reconstruction process, which enhances print monitoring and provides valuable insights into the quality of the printed object. Additionally, augmented reality tools, such as the HoloLens,[4] allow users to interact with and inspect the reconstructed model in a mixed-reality environment, further supporting process improvement and defect detection (printing type: nozzle-based).

Wasserfall et al. [42] an algorithm that for identifying failures involves capturing high-resolution images of each printed layer using a camera system integrated into the 3D printer. These images are stitched together to form complete layer visuals, which are segmented based on plastic or conductive ink extrusions using support vector machines (SVM). The system compares the segmented images with the expected layer layout extracted from the G-code to detect discrepancies such as insufficient or excessive ink extrusion and interruptions. If a defect is identified, the printing process is paused to prevent further errors. This real-time inspection ensures the quality of printed electronic circuits by closely monitoring the deposition of materials (printing type: nozzle-based).

Xu et al. [43] developed an algorithm for real-time defect detection in 3D construction printing using point cloud comparison. A 3D camera captures point clouds of each layer, compared against the CAD model using a cloud-to-plane (C2P) distance metric. Deviations trigger corrective actions,

[3] Red–green–blue.

[4] https://www.microsoft.com/en-us/hololens.

adjusting the printhead's motion to maintain accuracy (printing type: nozzle-based).

Bowoto et al. [11] proposed an image processing algorithm for real-time detection of defects such as porosity and cracks in printed layers. The system compares real-time images with a CAD model, using grayscale conversion, thresholding, and K-means clustering to measure defect regions, determining if they are within acceptable limits or if printing should be stopped (printing type: nozzle-based).

Shen et al. [20] designed an algorithm to detect surface defects by comparing the contours of printed objects with theoretical contours derived from the 3D model's point cloud. Images are captured at intervals, and contours are extracted using image processing. Discrepancies below a similarity threshold flag defects for early detection (printing type: nozzle-based).

Kopsacheilis et al. [44] introduced a visual quality control system using RGB-D cameras and point cloud data. The system compares the real-time geometry of printed parts with theoretical models generated from G-code, detecting dimensional deviations in the layer structure without interrupting the printing process (printing type: nozzle-based).

Petsiuka and Pearce [4] developed an algorithm that monitors 3D printing layer by layer, focusing on global and local parameters. The system detects height issues, compares global shapes with G-code trajectories, and performs local texture analysis to identify anomalies, addressing defects by modifying the G-code or pausing the print (printing type: nozzle-based).

Patil et al. [10] proposed an image processing algorithm for detecting defects and measuring features in laser additive manufacturing. Grayscale images are processed using Gaussian filters, morphological operations, and Canny edge detection to measure dimensions and detect surface defects within a 1.5 to 3.5% error range (printing type: light-induced).

Petsiuka and Pearce [5] also developed an algorithm to detect anomalies in 3D printing by comparing visual features of each layer with synthetic reference images generated in Blender. The system uses Histograms of Oriented Gradients (HOG) to calculate similarity metrics and detect errors like infill defects or layer shifts (printing type: nozzle-based).

Forte et al. [8] created the DaR3D[5] system, which uses image processing to detect slippage defects during 3D printing. Images captured at intervals are compared with previously stored images using the Normalized Root Mean Squared Error (NRMSE) algorithm. Deviations beyond thresholds indicate slippage, triggering user alerts (printing type: nozzle-based).

Rahmani Dabbagh et al. [45] proposed a machine learning–based algorithm to optimize 3D printing parameters. A gradient boosting regression model predicts printing outcomes based on temperature, pressure, and design complexity, helping users optimize parameters and reduce material waste and trial-and-error (printing type: nozzle-based).

Rill-García et al. [46] presented an anomaly detection algorithm for 3D concrete printing, using RGB cameras for image acquisition and deep learning–based segmentation. The system identifies geometrical anomalies and classifies the concrete's texture into categories, detecting material-related defects during the print (printing type: nozzle-based).

Zhao et al. [47] introduced a surface defect detection algorithm using 3D point clouds. The MBH-INRoPS[6] feature descriptor enhances accuracy, while Euclidean clustering identifies defects, effectively separating defect regions from noise (printing type: nozzle-based).

Binder et al. [48] developed a framework linking thermal images with 3D models in fused filament fabrication (FFF). The system monitors temperature distribution to detect defects like warping and over-extrusion, allowing real-time adjustments to printing parameters (printing type: nozzle-based).

Oleff et al. [1] introduced an algorithm that uses dark-field illumination to capture high-contrast images of printed layers. Anomalies are detected using unsupervised machine learning techniques, such as isolation forests, to compare features of each layer with normal patterns, providing real-time monitoring across subareas (printing type: nozzle-based).

### 4.2 Classical no-reference methods

In no-reference methods, defect detection does not rely on comparing the printed part to reference data or its intended design. Instead, it focuses on identifying features that are independent of the specific part being printed, meaning the design itself is not a factor in detection. Typically, visual indicators suggest potential printing issues to identify failures. Below, we present papers that use classical, no-reference methods to detect defects in printed or in-progress parts.

Baumann and Roller [49] captured video frames during FFF builds and used image segmentation and frame differencing to detect layer misalignments or part detachment. Their system checked for shifts in the printed object's position between consecutive layers and could flag "detachment" or "deformation" events early. Heuristic techniques have also been used—for example, placing a bounding box around the printed region and tracking its centroid can reveal

[5] Detect and recognizing 3D printing.
defects.

[6] Improved normal rotated projection statistics.

a "missing extrusion" if the deposited material suddenly shrinks or shifts off-center. These vision-based methods rely on changes in shape or color over time (without any ground truth), and are relatively simple but limited to detecting gross deviations or specific failure modes (printing type: nozzle-based).

Fastowicz and Okarma [50] proposed an algorithm for assessing 3D print quality using texture analysis based on the Gray-Level Co-occurrence Matrix (GLCM) and Haralick features. The method converts images of 3D-printed objects into grayscale, then calculates the GLCM in four directions—horizontal, vertical, and two diagonal orientations. Homogeneity in texture is assessed using Haralick features, which analyze pixel intensity relationships to identify structural defects. Peaks and oscillations in homogeneity values indicate defects, with low-quality prints displaying reduced texture consistency. This approach allows continuous quality monitoring during printing without the need for predefined reference images (printing type: nozzle-based).

Wu et al. [23] introduced an image classification method to detect defects during the 3D printing process. Their system captures images during the infill printing stage and extracts features such as grayscale mean, standard deviation, and pixel counts above a threshold. These features are divided into sections for detailed analysis. The system classifies images as defective or non-defective using Naive Bayes Classifier and J48 Decision Trees (printing type: nozzle-based).

Yi et al. [51] integrated machine vision with statistical process control to enhance quality. Images of each printed layer are captured using a digital camera and processed to extract contour and area information for statistical analysis. Control charts are used to detect deviations from expected geometric parameters, enabling real-time detection of surface defects and irregularities. The system has a monitoring accuracy of 0.5 mm, ensuring better quality control in additive manufacturing (printing type: nozzle-based).

Okarma et al. [52] applied Structural Similarity (SSIM) metrics to assess 3D print quality without requiring a reference model. Images of the 3D-printed objects are analyzed for local self-similarity to detect distortions indicative of lower quality. Modified metrics, Complex Wavelet SSIM (CW-SSIM) and Structural Texture Similarity (STSIM), enhance defect detection sensitivity. The algorithm divides images into blocks, calculates similarity scores, and averages them to classify overall print quality. While SSIM alone may yield inconsistent results, CW-SSIM and STSIM provide more reliable assessments (printing type: nozzle-based).

Okarma and Fastowicz [53] proposed a novel visual quality assessment approach for 3D-printed surfaces using image entropy. The algorithm assumes regular patterns in printed objects exhibit low entropy values, while distortions increase entropy, indicating potential quality issues. To address color dependency, the method combines local entropy calculations with their variance across the hue component in the HSV color space and the RGB channels. This combined entropy approach effectively distinguishes between different quality levels in printed surfaces, independent of filament color (printing type: nozzle-based).

Shen et al. [54] developed a multi-view vision detection system using a CCD camera to capture images of the printed part's outer surface. After image preprocessing to enhance contrast and reduce noise, the system applies a dual-kernel detection technique based on morphological image processing. Rectangle and square kernels cover horizontal and vertical directions to detect potential defects. Contours are analyzed using the minimum enclosing rectangle (MER) method, and defects are classified by aspect ratio and area distribution, diagnosing issues like over-extrusion or mechanical problems (printing type: nozzle-based).

Kazemian et al. [55] designed a real-time quality monitoring system for extrusion processes using computer vision techniques. The system captures video frames of freshly extruded layers and measures their width, comparing it to a predetermined target width. Techniques like Gaussian blurring and Otsu's binarization segment the extruded layer, and contours are extracted to compute the average width across several frames. The system also features a closed-loop feedback mechanism, automatically adjusting the extrusion rate to maintain print quality, regardless of material property variations (printing type: nozzle-based).

Okarma and Fastowicz [56] adapted full-reference image quality assessment (IQA) metrics for automatic evaluation of 3D-printed surfaces. The system captures images of printed layers during the manufacturing process, detecting distortions and assessing quality. IQA metrics like Structural Similarity Index (SSIM) and Feature Similarity Index (FSIM) compare segments of the printed surface with expected quality, assuming higher similarity values indicate better quality. Images are processed by converting to grayscale, adjusting contrast, and analyzing fragments. The system successfully classifies prints into quality levels, achieving high accuracy in distinguishing quality variations (printing type: nozzle-based).

Fastowicz et al. [57] developed a method for objective 3D-printed surface quality assessment using entropy analysis of depth maps obtained from 3D scanning. Scanning creates detailed depth maps, which are processed to compute entropy values—a statistical measure of randomness. Lower entropy values correspond to high-quality surfaces with regular patterns. The method incorporates local entropy variance to account for non-uniformities in depth maps, allowing for reliable surface quality classification. The system effectively distinguishes between high and low-quality samples, providing a practical solution for online monitoring (printing type: nozzle-based).

In another work, Okarma and Fastowicz [58] applied various computer vision techniques to conduct non-destructive quality assessments of 3D-printed objects. Texture analysis using GLCM extracts features for classifying surface quality, while image entropy detects surface irregularities. Additionally, the Hough Transform identifies straight lines on printed objects. This real-time system uses strategically placed cameras to monitor the printing process without interrupting it, effectively identifying defects and assessing surface quality (printing type: nozzle-based).

Fastowicz and Okarma [59] also proposed a method for assessing the quality of 3D-printed flat surfaces using image analysis. Photographs of printed samples are captured, and the Hough Transform is used to detect straight lines corresponding to filament layers. Preprocessing steps like brightness compensation and CLAHE enhance image quality, aiding line detection. By analyzing the average length of detected lines, the algorithm generates a quality metric that classifies samples into high and low-quality categories, independent of filament color (printing type: nozzle-based).

Okarma and Fastowicz [60] introduced a color-independent method for 3D-printed surface quality assessment using image entropy. Distorted surfaces exhibit increased entropy values, indicating irregularities. The algorithm combines local entropy calculations with their variance across color spaces (RGB and HSV), processing images to evaluate local entropy and classify print quality. The system detects surface defects regardless of filament color, providing reliable assessments during and after printing (printing type: nozzle-based).

Liu et al. [61] proposed an algorithm that integrates image processing techniques like textural analysis through GLCM for defect detection and a PID-based feedback control system for defect mitigation. The system adjusts machine parameters such as material flow rate and extruder temperature based on detected defects (printing type: nozzle-based).

Yan et al. [16] introduced a defect detection algorithm for FDM 3D printing, using traditional image processing techniques. The system captures images of printed layers with a monocular camera, extracting the stacked area using K-means clustering. A 2D Gabor wavelet transform detects wire drawing defects by analyzing texture differences in printed layers. The Hough line detection algorithm identifies defects, providing real-time detection to enhance the printing process (printing type: nozzle-based).

Zhou et al. [19] developed an algorithm for detecting surface defects like pits, bubbles, and bulges in ceramic 3D printing. The region of interest (ROI) is identified, and images are preprocessed using Gaussian filtering to reduce noise. Morphological operations preserve the object's shape and structure, while specific defects are detected based on their characteristics. Defects are classified by comparing their size, shape, and location to predefined thresholds using a dual-threshold approach (printing type: nozzle-based).

Mohr et al. [62] focused on developing a method for real-time defect detection during the LPBF. They used a combination of mid-wave infrared (MWIR) thermography and optical tomography to monitor the melt pool and identify process deviations. The thermography camera was used to analyze thermal signals and identify "time over threshold" (TOT) events, which indicate potential defects. The optical tomography camera provided additional data on the melt pool geometry and signal intensity. The results from these in situ monitoring methods were then compared to micro-X-ray computed tomography (μCT), a high-resolution ex situ method, to validate the effectiveness of their approach in detecting defects like lack of fusion and keyholes.

Mazzarisi et al. [63] discusses the use of infrared thermography as a method for real-time monitoring of the laser metal deposition (LMD) process. The research focuses on an ad hoc algorithm implemented in MATLAB to analyze the thermal data captured by an IR camera. This algorithm is used to extract key thermal metrics such as maximum temperatures, thermal gradients, and cooling rates. The study's findings are applied to understand the thermal behavior of different deposition strategies and their impact on the final product, with the goal of improving quality control in LMD manufacturing.

AbouelNour and Gupta [26] present a method for in-process defect detection in additive manufacturing by utilizing a multi-sensor approach. The study uses both optical imaging and infrared thermography to monitor the build process. The core of the work involves analyzing the acquired images to detect and characterize defects, such as hotspots, by evaluating metrics like average specimen temperature, global average hotspot temperature, total number of hotspots, perimeter, and surface area. This approach aims to provide a reliable way to monitor the quality of additively manufactured parts as they are being built.

De Santana et al. [25] evaluates an active thermography algorithm for detecting subsurface defects. The algorithm uses thermographic signal reconstruction, thermal contrast, and heat transfer principles to analyze heat flow in an object after it has been excited by a heat source. Any internal defects, such as voids or inconsistencies, disrupt the heat flow, causing a change in the surface temperature that can be captured by an infrared camera. The study also highlighted the significant effect of infill percentage on the heat transfer behavior of the workpieces, noting that samples with 100% infill showed more well-defined defective regions compared to those with 30% infill.

Höfflin et al. [64] focus on in situ defect detection during the LPBF process. The proposed method utilizes active thermography to monitor the melt pool and surrounding area. The study introduces a novel approach for detecting defects by analyzing the spatial temperature distribution in these thermographic images. It evaluates two specific algorithms, a gradient approach and a derivative approach, both designed to identify irregularities in the temperature profile that indicate potential defects. This work aims to provide a real-time quality control system for LPBF, ensuring the integrity of the printed parts.

Montinaro et al. [65] present a numerical and experimental study using a remote laser thermographic methodology called "Flying Laser Inner Probing Thermography" (FLIPT) to detect micrometric defects in metal additive manufactured (AM) parts. The authors employed a finite element analysis (FEA) to simulate the thermal behavior of a sample and optimize the parameters of the technique to enhance its sensitivity to defects. The study's results indicate that the technique is successful in identifying flaws. The authors propose that this method is suitable for integration into the AM manufacturing process for continuous in-line inspection.

In summary, full-reference methods detect defects by comparing the printed part to an ideal reference model or dataset, such as a CAD model or simulated data like STL files or G-code. In contrast, no-reference methods detect defects without relying on reference data or predefined models, instead focusing on identifying visual or structural anomalies within the printed part, independent of its design.

### 4.3 Comparative analysis of classical defect detection techniques

The classical approaches for defect detection in 3D printing have been extensively studied and implemented over the years. These methods primarily fall into two categories: "full-reference methods," which compare printed parts to a pre-defined ideal reference, and "no-reference methods," which analyze the printed part without relying on a specific reference model. While both categories have demonstrated success in defect detection, they exhibit unique advantages and limitations.

Full-reference methods rely on *comparison-based techniques*, utilizing CAD models, previous prints, or predefined structures as a reference. These approaches tend to offer *higher accuracy* in identifying *geometric defects*, layer misalignments, and incomplete depositions. However, they require the generation and storage of accurate reference models, making them less flexible for variable and highly customized 3D prints.

No-reference methods, on the other hand, leverage *statistical and machine vision techniques* to identify defects by analyzing texture, contour consistency, or material distribution without predefined reference data. These methods offer greater *adaptability* but might be *less precise* when detecting structural defects that deviate subtly from the expected geometry.

Table 2 summarizes the key characteristics of classic techniques for defect detection, focusing on the type of reference used, the extracted features, evaluation metrics, data format, input size, and inference time. This comparison highlights the diversity in data acquisition and analysis strategies, ranging from full-reference geometric comparisons to no-reference texture-based methods.

To provide a general indication of computational performance, an "Inference Time per Image" column has been added to the rightmost side of the table. These values are directly extracted from the referenced articles and should be interpreted with caution, as differences in hardware specifications, software implementations, and testing environments make direct comparisons unreliable. They are intended solely as rough indicators of computational cost. Notably, many studies do not report this value, possibly because the inherently slow pace of 3D printing allows ample time for image processing, especially when using high-performance vision hardware.

## 5 Modern techniques for defect detection

Both full-reference and no-reference approaches have been applied in modern defect detection methods. However, a statistical analysis of articles in this field indicates that researchers are increasingly focusing on no-reference methods. This shift may be attributed to the powerful capabilities of deep learning. The following sections will present a review on the papers within this category.

### 5.1 Modern full-reference methods

As this article has already covered how full-reference methods function, we will now shift to presenting works in this category that utilize deep learning.

Muktadir and Yi [15] introduced a machine learning algorithm using the PointNet neural network to detect defects in 3D-printed objects by analyzing point cloud data. The algorithm processes 3D images from CAD models and 3D scanners, converting them into point clouds. These point clouds are segmented and analyzed using the PointNet model, trained on both normal and defective data. This allows the system to classify and detect defects such as surface roughness and structural inconsistencies in real time, without relying on pre-existing reference images (printing type: nozzle-based).

Sun et al. [66] explored the application of both traditional machine learning and deep learning techniques in optimizing the bioprinting process. These algorithms model the relationships between printing parameters (e.g., nozzle diameter, extrusion pressure, and bioink viscosity) and the quality of bioprinted constructs. Deep learning techniques,

**Table 2** Comparative summary of classic techniques for defect detection

| Paper | Ref. type | Feature type | Metric used | Data format | Input size | Inference time per image |
|---|---|---|---|---|---|---|
| **Cheng et al.** [33] | FIR* | Surface geometry, contour deviation | Contour extraction + threshold-based classification | Grayscale image | NR** | NR |
| **Straub** [9] | FIR | RGB pixel-wise image differences | Aggregate pixel difference, average per-pixel difference, percentage of threshold-exceeding pixels | RGB image | NR | NR |
| **Hurd et al.** [34] | FIR | 2D layer comparison (top-down image) | Pixel-wise error (internal and external), thresholds | PNG/JPEG (mobile camera) | 1280 × 800 | 0.2 ~ 2.2 s |
| **Ceruti et al.** [35] | FIR | SURF feature points | Pixel-wise displacement/deviation threshold | Real camera image + STL | NR | NR |
| **Johnson et al.** [36] | FIR | Top-view visual geometry | Pixel-wise deviation from sliced reference images | PNG (camera + STL slices) | 2048 × 2048 pixels | NR |
| **Nuchitprasitchai et al.** [37] | FIR | Shape-based (2D shape vs. STL), 3D geometry | Shape difference (%), size difference (%) | PNG (CameraImage, STLImage) | 480 × 640 | Single-camera: ~ 6.5–9 s<br>Two-camera: ~ 38–74 s |
| **Straub** [38] | FIR | Visible-light 2D images from multiple perspectives; compared to reference models | Difference visualization and structural discrepancy detection | RGB images captured by fixed cameras | NR | NR |
| **Holzmond et al.** [12] | FIR | 3D geometric surface deviation | Point-wise Z deviation | 3D point clouds | Not explicitly in pixels | NR |
| **Lyngby et al.** [39] | FIR | Binary segmentation masks of expected vs. actual object layers | Error ratio | RGB image | NR | NR |
| **Delli et al.** [40] | FIR | Average RGB values per section of the image | Experimental error per section | RGB images | 640 × 480 | NR |
| **Malik et al.** [41] | FIR | Layer-wise 2D-to-3D reconstruction | No explicit numeric metric | RGB images | 13 MP | NR |
| **Wasserfall et al.** [42] | FIR | Classified pixel regions | Pixel-wise classification accuracy | RGB images | NR | ~ 1.5–1.6 s |
| **Xu et al.** [43] | FIR | Point cloud deviation | Cloud-to-Plane (C2P) distance metric | RGB-D images | 512 × 512 (Kinect depth resolution) | NR |
| **Bowoto et al.** [11] | FIR | Pixel intensity, pore distribution, contour irregularities, defect clusters via K-means clustering | Sum of squared Euclidean distance between defect points and cluster centers | RGB images | 1360 × 1024 pixels | 0.48 s |
| **Shen et al.** [20] | FIR | Contour shape | Differences in position, aspect ratio, and area of contours | RGB images | 1626 × 1236 pixels | NR |
| **Kopsacheilis et al.** [44] | FIR | Voxel-based spatial difference | Spatial change percentage between theoretical and actual point clouds | RGB-D images | NR | NR |
| **Petsiuka et al.** [4] | FIR | Layer geometry | Contour shape difference | RGB images | 1920 × 1080 pixels | NR |
| **Patil et al.** [10] | FIR | Deposition shape | Bounding box geometry for defect location, error | RGB images | NR | NR |

**Table 2** (continued)

| Paper | Ref. type | Feature type | Metric used | Data format | Input size | Inference time per image |
|---|---|---|---|---|---|---|
| **Petsiuka et al.** [5] | FIR | Contour and infill patterns | Pixel-wise deviation | RGB images | 1280 × 720 pixels | NR |
| **Forte et al.** [8] | FIR | Whole-frame grayscale pixel intensities | Normalized root mean square error, accuracy | Gray images | NR | NR |
| **Rahmani et al.** [45] | FIR | Average RGB values per image section | RGB difference error rate per region, prediction performance | RGB images | 640 × 480 pixels | NR |
| **Rill-García et al.** [46] | FIR | Geometry + texture | *F*-Score (segmentation: 90.6%, texture: 94%) | RGB image | 1280 × 960 pixels | NR |
| **Zhao et al.** [47] | FIR | MBH-INRoPS (3D) | Accuracy, recall, precision | 3D point cloud | 2048 × 2448 | NR |
| **Oleff et al.** [1] | FIR | First-order statistics, gradients, Fourier filters, eccentricity, dilated area, median absolute deviation | Imperfect area % (IA), imperfection density | Grayscale image | NR | NR |
| **Baumann et al.** [49] | NoR*** | Blob features, differential motion analysis | Detection rate | RGB image | 640 × 480 pixels | ~5 s |
| **Fastowicz et al.** [50] | NoR | Haralick features from GLCM | Peak-to-peak amplitude of homogeneity | Gray images | NR | NR |
| **Wu et al.** [23] | NoR | Mean, SD, and thresholded pixel counts per region | Classification accuracy | Gray images | 512 × 512 pixels | 0.3 s |
| **Yi et al.** [51] | NoR | Contour, cross-sectional area | SPC control charts (I-MR, Z chart), area deviation, accuracy | RGB and gray images | NR | NR |
| **Okarma et al.** [52] | NoR | SSIM, CW-SSIM, STSIM similarity maps | Mean similarity scores | Grayscale scanned and camera images | NR | NR |
| **Okarma et al.** [53] | NoR | Entropy | Combined quality indicator based on entropy and its variance (EV) | NR | NR | NR |
| **Shen et al.** [54] | NoR | Surface defects | Aspect ratio, area distribution, and pixel statistical value | NR | NR | NR |
| **Kazemian et al.** [55] | NoR | Shape-based features | Measures the width of the freshly extruded layer and compares it to a target width, accuracy | RGB images | 640 × 480 pixels | NR |
| **Liu et al.** [61] | NoR | Image textural features | Defect type and severity, accuracy | Gray images | 640 × 480 pixels | NR |
| **Yan et al.** [16] | NoR | Layer geometry | NR | Gray images | NR | NR |
| **Zhou et al.** [19] | NoR | Geometric features | Accuracy, recall rate, and precision | RGB images | 4000 × 3036 pixels | NR |
| **Mohr et al.** [62] | NoR | Time over threshold on thermographic image, and threshold on visible image | Compared to micro-X-ray computed tomography (μCT) | Visible + near infrared, mid-infrared | 4112 × 3012 pixels 192 × 176 pixels | NR |

**Table 2** (continued)

| Paper | Ref. type | Feature type | Metric used | Data format | Input size | Inference time per image |
|---|---|---|---|---|---|---|
| **Mazzarisi et al.** [63] | NoR | Thermal gradient | Metallographic analysis | Thermal camera | 320×256 pixels | NR |
| **AbouelNour et al.** [26] | NoR | Hotspot temperature | Correlation between the global average hotspot temperature and the total number of embedded defects | Optical and thermal images | Optical: 375×165<br>Thermal: 160×120 | NR |
| **De Santana et al.** [25] | NoR | Thermal amplitude, time constant, and thermal contrast | Sensitivity to defect depth | Thermographic images | NR | NR |
| **Höfflin et al.** [64] | NoR | Thermal gradient | Metallographic analysis | Infrared camera | 160×160 pixels | Gradient approach: 3.1 s for 2000 frames<br>Derivative approach: 3.9 s for 2000 frames |
| **Montinaro et al.** [65] | NoR | Mean and SD of temperature distribution in a region of interest | Comparison of numerical results and real examples | Infrared camera | 640×512 pixels | NR |

The table outlines the reference type, extracted features, evaluation metrics, data format, input image size, and inference time (if reported) for each method

*FIR: Full reference; **NR: not reported; ***NoR: No reference

like CNNs, are used for real-time image analysis to detect defects and anomalies. The models predict outcomes such as fiber diameter, shape fidelity, and cell viability, providing dynamic feedback to optimize printing parameters and improve the quality of bioprinted structures (printing type: nozzle-based).

Niu et al. [67] proposed a semi-Siamese convolutional neural network that takes as input both the planned model image and the camera-captured image from the 3D printer, and outputs a pixel-wise defect map. By learning to directly compare these two visual domains, the model demonstrates strong robustness to variations in camera angles and lighting conditions, achieving an F1-score greater than 0.9 and processing each layer image in approximately 0.5 s on a standard laptop (printing type: nozzle-based).

Charia et al. [68] addressed stringing defects by fine-tuning a convolutional neural network (CNN) to detect stray "spaghetti" filament. Their approach involves subtracting a synthetic reference silhouette, rendered directly from the G-code, from the real camera image to isolate extraneous material. This method generates a color-coded error map in real time and operates without the need for specialized hardware. The use of a simple binary reference image enhances robustness against variations in lighting conditions and camera configurations, making the system highly practical for standard 3D printing environments (printing type: nozzle-based).

## 5.2 Modern no-reference methods

As this article has already discussed the workings of no-reference methods, we will now focus on introducing works in this category that utilize deep learning.

Caggiano et al. [14] presented a bi-stream Deep Convolutional Neural Network (DCNN) for detecting defects in the selective laser melting (SLM) process. Their approach analyzes real-time images of both powder layers and part slices, capturing surface patterns that indicate defects due to improper process conditions. The DCNN extracts multi-level features, and a softmax classifier identifies defect patterns. This approach effectively correlates irregularities in powder layers with defects in part slices to ensure part quality (printing type: light-induced).

Jin et al. [69] proposed a Convolutional Neural Network (CNN)–based algorithm to classify 3D printing quality into under-extrusion, good-quality, and over-extrusion categories. The CNN, trained on labeled images, monitors real-time printing and automatically adjusts the flow rate to correct printing conditions, iteratively ensuring print quality with minimal human intervention (printing type: nozzle-based).

Razaviarab et al. [70] developed a closed-loop machine learning system that optimizes additive manufacturing processes in real time. After offline training with sensor data, the system uses deep CNNs to monitor the print's condition and autonomously adjust parameters like laser power or material flow to prevent defects (printing type: light-induced).

Banadaki et al. [71] proposed an algorithm that involves a deep convolutional neural network (CNN) that processes images of each printed layer to detect defects, such as overfill or voids, which can degrade the structural integrity of the printed part. The CNN is trained on images from various printing speeds and temperatures to classify the quality of prints into five grades. The system monitors the AM process in real time, detecting anomalies and predicting failure risks early. If the quality deviates from acceptable levels, the feedback mechanism adjusts print parameters—such as extrusion speed and temperature—automatically to correct the process (printing type: nozzle-based).

Garfo et al. [72] used the MobileNet-SSD model for defect detection in 3D-printed parts. By processing real-time images and identifying surface defects such as roughness and cracks, the system achieves high accuracy in localizing defective areas, benefiting from its efficient feature extraction architecture (printing type: nozzle-based).

Baumgart et al. [73] optimized CNN architecture using depthwise-separable convolutions to detect defects like delamination during laser-powder bed fusion (L-PBF). Thermographic images captured during printing are analyzed by the CNN, providing defect detection with minimized computational costs (printing type: light-induced).

Paraskevoudis et al. [74] introduced a deep CNN for detecting stringing defects in 3D printing, using live video footage. The model outputs bounding boxes around detected defects and alerts the user or stops the print process if the probability of a defect exceeds a set threshold, prioritizing speed and accuracy (printing type: nozzle-based).

Farhan Khan et al. [75] developed a CNN-based system that analyzes top-view images of printed layers in real time to detect defects like weak infill or misalignment, pausing the process if a defect is detected, thus reducing material waste and improving reliability (printing type: nozzle-based).

Brion et al. [76] proposed an algorithm that utilizes a deep learning–based object detection approach using the YOLOv3 model to identify warp deformation during printing. Images captured during the printing process are analyzed to detect warping in real time. The model calculates key metrics, such as the area and volume of warped regions, the number of detections, and the confidence of predictions. These metrics are used to assess the severity of the deformation, which informs corrective actions. The system intervenes by adjusting print parameters such as bed temperature and fan speed to prevent further warping. Additionally, insights from detected warp patterns are applied to future prints to refine the printing process and reduce the likelihood of recurrence (printing type: nozzle-based).

Brion and Pattinson [77] utilized a multi-head neural network to detect and correct errors in real time during 3D printing. This system monitors parameters like flow rate and Z offset, adjusting them dynamically to ensure consistent quality across different materials and geometries (printing type: nozzle-based).

Nguyen et al. [78] proposed a hybrid machine learning model combining an MLP and CNN to optimize 3D printing. The MLP manages physical parameters, while the CNN analyzes geometric properties, improving process efficiency by learning from simulation data (printing type: nozzle-based).

Zhang et al. [17] employed a CNN, FDMNet, to detect defects like interlayer stripping in multi-axis 3D printing. A CCD camera captures images during printing, and the CNN, trained with data augmentation, classifies prints with a high accuracy of 83.1% (printing type: nozzle-based).

Cao et al. [79] incorporated an attention module into a YOLOv8 model to detect extrusion irregularities—such as under-extrusion and over-extrusion—during the 3D printing process. Their real-time vision system was directly integrated into the printer's control loop, enabling automatic adjustment of the extrusion speed when a flow defect was detected. This closed-loop approach demonstrates the feasibility and practicality of no-reference defect detection for immediate corrective intervention in FFF processes, significantly enhancing print reliability and consistency (printing type: nozzle-based).

Wang et al. [18] enhanced the YOLOv8 model for real-time defect detection in additive manufacturing, integrating a coordinate attention mechanism and EIOU loss function to detect defects like scratches and holes, achieving high-speed, accurate defect identification (printing type: nozzle-based).

Hu et al. [80] also reported the application of an enhanced YOLOv8 deep learning algorithm for defect detection in 3D printing, further demonstrating the potential of advanced object detection models for real-time monitoring and quality assurance in additive manufacturing (printing type: nozzle-based).

Aksoy and Ozsoy [81] achieved approximately 97% classification accuracy on a diverse image dataset of common FDM print failures by utilizing a MobileNetV3 model, highlighting the effectiveness of lightweight CNN architectures for automated error detection. These CNN-based approaches learn to recognize a combination of texture and shape features—such as the roughness of a warped edge or the wispy patterns of stringing—directly from the training images, making them highly sensitive to the specific defects they were trained to detect. Beyond simple classification, object detection networks have also been employed to locate defects spatially within images, further enhancing the practicality of deep learning methods for real-time monitoring and quality control in additive manufacturing (printing type: nozzle-based).

Singh et al. [82] utilized a Data-Efficient Image Transformer (DeiT) architecture, fine-tuned to recognize three major types of print quality issues: bed warping, layer delamination, and gaps in raster infill lines. By attending to the overall structural patterns within an image, the transformer-based system was able to accurately identify these defects across a range of print geometries. Early results suggest that transformer models, particularly when pretrained on large datasets, can achieve high classification accuracy for FFF print anomalies, comparable to that of Convolutional Neural Networks (CNNs). However, due to their greater data and computational requirements, lightweight CNN-based solutions remain preferable for real-time defect detection applications (printing type: nozzle-based).

Szymanik et al. [83] present a method for detecting and identifying defects in 3D-printed dielectric structures using thermographic inspection and deep neural networks (DCNNs). The approach involves applying a heat pulse to the object and using an infrared camera to capture a sequence of thermal images as the object cools down. These images are then analyzed using two methods: a correlation coefficient analysis to find the area of interest, and a deep convolutional neural network (DCNN) for classification. The DCNN is trained to classify the presence, diameter, and depth of various defects, which are introduced into the 3D-printed samples. The key contribution is the hybrid approach that combines signal analysis with deep learning to achieve high accuracy in detecting and characterizing defects in a non-contact and non-destructive manner.

### 5.3 Comparative analysis of modern defect detection techniques

Modern defect detection techniques in 3D printing leverage advanced computational methods, including "machine learning, deep learning" and "real-time monitoring systems." Unlike classical methods, these approaches do not solely rely on predefined reference models or handcrafted features; instead, they can autonomously learn feature representations and make intelligent predictions.

Machine learning and deep learning–based methods offer enhanced precision and adaptability in defect detection. They utilize vast datasets to train models that can detect and classify defects based on historical print data. *Convolutional Neural Networks (CNNs)*, *autoencoders*, and *transformers* are some of the most commonly used architectures in modern defect detection.

These approaches outperform classical methods in handling complex and large datasets, but they also require significant computational power and large labeled datasets for training.

Table 3 summarizes the key characteristics of modern techniques for defect detection, focusing on the type of reference used, the extracted features, evaluation metrics, data format, input size, and inference time. This comparison highlights the diversity in data acquisition and analysis strategies, ranging from full-reference geometric comparisons to no-reference texture-based methods.

To offer a rough estimate of computational performance, an "Inference Time per Image" column is included on the right side of the table.

Beyond computational efficiency, one of the key challenges in machine learning–based defect detection is the annotation of training data. Given the high variability of part geometries and defect types in AM, constructing large, labeled datasets is often impractical. Consequently, recent approaches increasingly rely on unsupervised or one-class learning techniques, which are trained solely on normal (defect-free) samples. This reduces the annotation burden and improves adaptability across different printing scenarios.

## 6 Comparison of defect detection algorithms

### 6.1 Classical algorithms versus modern algorithms

Classical pattern classification methods separate feature extraction and classification, relying on manually designed algorithms to extract features, followed by classifiers. These approaches are limited by the quality of hand-engineered features. In contrast, modern deep learning algorithms integrate feature extraction and classification into a single, learning-based process. This automatic feature learning significantly improves performance and scalability, especially with complex and large datasets, driving advancements in fields like image recognition and defect detection. Table 4 compares these two approaches.

### 6.2 Full-reference algorithms versus no-reference algorithms

In full-reference methods, defect detection is performed by comparing the printed part to an ideal reference model or dataset. This reference could be a CAD model, a previously printed ideal part, or simulated data (such as STL files or G-code). While, in no-reference methods, defect detection does not depend on any reference data or predefined models. Instead, the method focuses on identifying visual or structural anomalies within the part being printed, independent of the specific design. Table 5 compares these two different approaches.

**Table 3** Comparative summary of modern techniques for defect detection

| Paper | Ref. type | Model type | Metric used | Data format | Input size | Inference time per image |
|---|---|---|---|---|---|---|
| **Muktadir et al.** [15] | FlR* | PointNET | Accuracy | Point cloud | NR* | NR |
| **Sun et al.** [66] | FlR | CNN | Detection accuracy, fiber continuity, regularity, and surface uniformity | NR | NR | NR |
| **Niu et al.** [67] | FlR | Semi-Siamese convolutional neural network | Accuracy, macro-F1-score, precision, recall, IOU, and F1-score for each class | A pair of 2D images for a single layer | NR | 0.419 s |
| **Caggiano et al.** [14] | NoR*** | MobileNet-SSD | Mean defective condition, accuracy | NR | 160 × 160 pixels | NR |
| **Jin et al.** [69] | NoR | CNN | Accuracy | RGB images | 224 × 224 pixels | NR |
| **Razaviarab et al.** [70] | NoR | CNN | Classification accuracy | RGB images | NR | NR |
| **Banadaki et al.** [71] | NoR | CNN | *F*-score, sensitivity, precision, specificity, and accuracy | RGB images | 600 × 600 pixels | NR |
| **Garfo et al.** [72] | NoR | MobileNet-SSD | Mean average precision, intersection-over-union, accuracy | RGB images | 300 × 300 pixels | NR |
| **Baumgart et al.** [73] | NoR | CNN | Balanced accuracy, class averaged sensitivity, precision, Cohen's Kappa score | Thermographic images | 270 × 270 images | NR |
| **Paraskevoudis et al.** [74] | NoR | CNN | Precision, recall, F1-score, and average precision | RGB image | 300 × 300 pixels | 71 ms |
| **Farhan Khan et al.** [75] | NoR | CNN | Accuracy and uniformity | RGB images | NR | NR |
| **Brion et al.** [76] | NoR | YOLOv3 | Precision, recall, F1-score | RGB images | 1280 × 720 pixels | NR |
| **Brion et al.** [77] | NoR | Multi-head NN | Accuracy | RGB images | 224 × 224 images | NR |
| **Nguyen et al.** [78] | NoR | CNN | Mean square error, mean absolute error | RGB images | NR | NR |
| **Zhang et al.** [17] | NoR | FDMNet | Accuracy, sensitivity, specificity, ROC curve | Gray images | 227 × 227 pixels | 1.5 μs |
| **Cao et al.** [79] | NoR | YOLOv8 | Mean average precision | RGB images | 640 × 480 pixels | 80 ~ 480 ms |
| **Wang et al.** [18] | NoR | YOLOv8 | Precision, recall, average precision, mean average precision, accuracy | RGB images | 640 × 640 pixels | 13.9 ms |
| **Hu et al.** [80] | NoR | YOLOv8 | Precision, recall, mean average precision, F1-score | RGB images | 3072 × 2048 pixels | 10.8 ms |
| **Aksoy et al.** [81] | NoR | CNN | Accuracy, precision, recall, and F1-score | RGB images | 224 × 224 pixels | NR |
| **Singh et al.** [82] | NoR | CNN | Weighted classification accuracy, accuracy, precision, recall, F1-score | RGB images | 224 × 224 pixels | 0.1121 s |
| **Szymanik et al.** [83] | NoR | CNN | Accuracy | Thermographic images | NR | NR |

The table outlines the reference type, extracted features, evaluation metrics, data format, input image size, and inference time (if reported) for each method

*FlR: Full reference; **NR: not reported; ***NoR: No reference

**Table 4** Comparing the pros and cons of the classical and modern, deep learning–based approaches to pattern classification

| | | |
|---|---|---|
| Pros | | |
| Aspect | Classical algorithm | **Modern, deep learning–based algorithm** |
| Transparency and interpretability | Highly interpretable due to manual feature extraction and predefined algorithms | Models are often seen as "black boxes" and lack transparency |
| Domain expertise integration | Allows for the integration of domain-specific knowledge into feature extraction | Automatically learns features from data without needing domain-specific expertise |
| Computational efficiency | Efficient with smaller datasets and less computationally demanding, suitable for real-time or low-resource environments | Computationally intensive, requiring significant resources for training, especially on large datasets |
| Automatic feature learning | Manual feature extraction is necessary, which can be time consuming and may not capture all relevant patterns | Automatically learns relevant features during training, reducing the need for manual feature engineering |
| Scalability | Limited scalability for complex or high-dimensional data, as performance heavily depends on feature extraction quality | Scales well with larger datasets and complex data, improving performance as more data is provided |
| Versatility across domains | Requires significant customization for different domains or applications | Highly adaptable and versatile across different tasks, such as image recognition, speech processing, and more |
| Cons | | |
| Aspect | Classical approach | **Modern, deep learning–based approach** |
| Performance on complex data | Struggles with complex, high-dimensional data, requiring extensive feature engineering for good performance | Excels in handling complex, high-dimensional data, especially in tasks like image and speech recognition |
| Dependency on feature engineering | Performance is highly dependent on the quality of hand-engineered features, making it a bottleneck | Eliminates the need for manual feature extraction, though it requires large amounts of labeled data for optimal performance |
| Data requirements | Can work with smaller datasets, though feature engineering is essential | Requires large, labeled datasets and significant computational power, making it less suitable for small-scale tasks |
| Risk of overfitting | Less prone to overfitting with simpler models, though performance may be limited | Prone to overfitting if not properly regularized or if there is insufficient training data |
| Interpretability | Models are easier to interpret and explain due to manually designed features and classification rules | Deep learning models are difficult to interpret and often viewed as black boxes |

**Table 5** Comparing the full-reference and no-reference methods

| Aspect | Full-reference methods | No-reference methods |
|---|---|---|
| Reference dependence | Relies on a reference model (e.g., CAD, STL) | No reference model required |
| Detection approach | Compare the print to an ideal reference | Focuses on detecting visual or structural anomalies |
| Accuracy | High accuracy due to comparison with ideal | Less precise, focuses on generalized defect indicators |
| Setup complexity | Requires generation and storage of reference models | Easier setup, no model creation required |
| Application | Best for controlled, precision environments | Suitable for flexible or varied manufacturing tasks |
| Examples of use | Geometric errors, misalignment, extrusion issues | Surface defects, texture inconsistencies, cracks |
| Pros | High reliability, suitable for precision parts | Adaptable, low setup requirements |
| Cons | Time consuming, inflexible for variable designs | Less accurate, may miss subtle or small defects |

**Table 6** Evaluation results of different algorithms methods

| Defect detection method: classic, full-reference | | |
|---|---|---|
| **Paper** | **Defect type or measurement** | **Evaluation result** |
| **Patil et al.** [10] | Dimension measurement | Error: 1.5 ~ 3.5% |
| **Forte et al.** [8] | Slippage in prints | Accuracy: 89.6% |
| **Dabbagh et al.** [45] | Extrusion defects | Prediction performance: 95.4% |
| **Rill-García et al.** [46] | Lines separating of layers<br>Material texture classification | *F*-score: 91%<br>*F*-score: 94% |
| **Zhao** [47] | Hump<br>Collapse<br>Poor bridging<br>Collapse and poor bridging<br>Hump and poor ridging<br>Hump and collapse | Accuracy: 99.89%<br>99.94%<br>99.68%<br>99.53%<br>99.66%<br>99.80% |
| **Defect detection method: classic, no-reference** | | |
| **Paper** | **Defect type** | **Evaluation result** |
| **Wu et al.** [23] | Infill defects | Accuracy: 95.51% |
| **Yi et al.** [51] | Counter profile | Accuracy: 0.5 mm |
| **Kazemian et al.** [55] | Extrusion width variations | Accuracy: within ± 1.7 mm |
| **Okarma et al.** [56] | Surface quality distortions | Accuracy: 96.8% |
| **Fastowicz et al.** [57] | Surface quality distortions | Accuracy: 90.5% |
| **Okarma et al.** [58] | Surface quality distortions | Accuracy: 96.8% |
| **Fastowicz et al.** [59] | Surface quality distortions | Accuracy: 79.5% |
| **Liu et al.** [61] | Defects of under-fill | Accuracy: 85% |
| **Zhou et al.** [19] | Surface defects | Accuracy: 97.20% |
| **Defect detection method: modern, full-reference** | | |
| **Paper** | **Defect type** | **Evaluation result** |
| **Muktadir et al.** [15] | Surface defects | Accuracy: 87.50% |
| **Defect detection method: modern, no-reference** | | |
| **Paper** | **Defect type** | **Evaluation result** |
| **Caggiano et al.** [14] | Surface defects | Accuracy: 99.40% |
| **Jin et al.** [69] | Under-extrusion, over-extrusion | Accuracy: 98.00% |
| **Razaviarab et al.** [70] | Surface defects | Accuracy: 100% |
| **Garfo et al.** [72] | Surface defects | Accuracy: 80.00% |
| **Baumgartl et al.** [73] | Delamination and splatter | Accuracy: 96.80% |
| **Paraskevoudis et al.** [74] | Stringing | F1-Score: 0.82 on training data |
| **Farhan Khan et al.** [75] | Infill patterns | Accuracy: 84.00% |
| **Zhang et al.** [17] | Interlayer stripping | Accuracy: 83.10% |
| **Wang et al.** [18] | Surface defects | Accuracy: 91.05% |
| **Niu** [67] | Surface defects | F1-Score: 0.9 |

### 6.3 Objective comparison of defect detection algorithms

Objectively comparing the presented methods poses significant challenges. While some studies report quantitative performance metrics, others offer only qualitative assessments, and direct comparisons are further complicated by variations in printer hardware, defect types, and dataset characteristics. Nevertheless, Table 6 provides a summary of the reported objective results across different studies.

The lack of a standardized dataset and the use of local datasets for algorithm evaluation prevent a fair and accurate comparison of the accuracy of different algorithms. As a result, comparing the accuracy values reported by various algorithms would not be entirely fair or reliable. This highlights the necessity of creating a comprehensive and publicly available dataset for benchmarking and comparing defect detection algorithms. However, the diverse approaches taken by different researchers to solve the problem make it highly challenging to develop a dataset that can adequately meet the needs of all algorithms.

## 7 Real-time feedback systems

Real-time feedback systems in 3D printers can be categorized based on the type of *feedback signals* they use and the *control algorithms* they implement.

### 7.1 Classification of real-time feedback systems

- Sensor-based feedback systems: optical (cameras), thermal (infrared), acoustic (vibrations), and pressure sensors.
- Data processing and signal interpretation: techniques such as edge detection, Fourier analysis, and AI-based anomaly detection.
- Control algorithm taxonomy: PID control, adaptive control, and AI-driven predictive control.

### 7.2 Types of feedback signals used in defect detection

- Geometric feedback: vision-based tracking for layer misalignment.
- Thermal feedback: infrared sensors detecting overheating or under-sintering.
- Acoustic and vibration feedback: detecting mechanical inconsistencies via sound patterns.

### 7.3 Control algorithms for defect mitigation

- PID-based control: proportional-integral-derivative adjustments.
- Fuzzy logic control: adaptive, rule-based error correction.
- Machine learning control: predictive AI models for defect pre-emptive correction.

Table 7 shows a comparison between different feedback systems.

Among them, real-time feedback, based on visual perception, play a vital role in 3D printing by integrating machine vision and feedback loops to dynamically adjust the printing process, preventing the propagation of defects. The inclusion of these mechanisms significantly improves both print quality and efficiency.

In [69], the system identifies errors like insufficient material flow or misalignment and implements real-time corrections. Parameters such as flow rate, lateral speed, Z-offset, and hotend temperature are adjusted dynamically, with G-code commands updated on the fly to optimize the ongoing print. Similarly, [77] employs a multi-head CNN trained on extensive datasets to detect and correct multiple parameters in real time, such as print speed and flow rate. These adjustments ensure optimal print outcomes across various materials and printer setups.

The system in [78] uses real-time data analysis, guided by machine learning models, to optimize printing parameters. Adjustments to extrusion rates and speeds are reflected through G-code modifications, enhancing overall efficiency. Article [59] discusses the use of real-time quality assessments, where filament feed rates and print speeds are adjusted to meet desired specifications. By using image entropy as a quality metric, the system fine-tunes parameters based on surface characteristics.

In [57], a depth map–based quality assessment system triggers G-code adjustments, further refining print outcomes. The system can modify printer settings, such as layer height and head calibration, based on detected defects. [38] focuses

**Table 7** Comparison of feedback systems in 3D printers

| Feedback type | Detection mechanism | Control method | Advantages | Limitations |
|---|---|---|---|---|
| Optical | Image analysis | AI-based correction | High accuracy | Requires high computing power |
| Thermal | Infrared monitoring | PID/fuzzy logic | Effective for overheating | Limited for small-scale defects |
| Acoustic | Sound pattern recognition | Adaptive AI | Detects mechanical faults | Limited dataset availability |

on identifying discrepancies in prints and dynamically adjusts printer settings through recalibrations of the print head and layer height, improving quality through continuous feedback.

The feedback mechanism in [70] relies on a closed-loop system to automatically adjust G-code commands. The system can alter laser scanning parameters or material flow in response to detected defects, improving the quality of the final print. Meanwhile, [18] leverages cloud-based monitoring for real-time defect analysis, enabling immediate G-code adjustments and continuous quality control.

Article [33] shows how imaging feedback drives adjustments to material flow rates, compensating for previously detected defects. In [43], a phased feedback mechanism detects defects and provides corrective feedback for subsequent layers, implementing adjustments such as angle modification and material refeeding. [66] underscores the importance of in situ monitoring, using machine learning models to detect anomalies in real time and initiate corrective actions. Lastly, [55] discusses how real-time monitoring assesses extrusion quality by detecting issues like over-extrusion or under-extrusion, providing corrective signals to enhance print quality.

### 7.4 Reinforcement learning for closed-loop control

Recently, reinforcement learning (RL) has gained attention as a promising framework for closed-loop control in additive manufacturing, particularly in simulated environments. RL enables the agent (e.g., the printer controller) to learn optimal printing strategies by interacting with a simulated or real process environment and receiving feedback in the form of rewards or penalties. This is especially useful in dynamic or non-linear processes such as layer deposition, temperature regulation, or defect correction.

Some efforts employ RL (e.g., Q-learning) to adaptively manage toolpath and orientation planning in fused deposition modeling (FDM), reducing support material use, print time, and surface roughness compared to traditional genetic-algorithm approaches [84]. Reinforcement learning has also been used to control metal additive processes such as laser-directed energy deposition by tuning laser power and scan speed to maintain desirable melt-pool depths in real time—without prior data or static models [85].

In parallel, closed-loop architectures using deep reinforcement learning—such as deep Q-learning or PPO—have been integrated with vision or sensor feedback to monitor and correct defects like over- or under-extrusion. For instance, vision-aware RL controllers trained in simulation can adjust extrusion parameters in real time with minimal sim-to-real gap, significantly enhancing print consistency and defect mitigation [86]. Additionally, hybrid RL frameworks coupled with multi-objective optimization techniques (e.g., neural nets, topology optimization) have yielded 15–25% reductions in material and time use and decreased defect rates by up to 30% in validated production workflows [87]. Overall, RL provides a versatile, dynamically adaptive approach for real-time process control, defect reduction, and parameter tuning across both FDM- and metal-based additive manufacturing.

### 7.5 Future directions

- Multi-sensor fusion: combining various sensors for better accuracy.
- Edge processing: reducing latency by performing computations locally.
- Self-learning adaptive systems: continual improvement of models through real-time feedback data.

By integrating advanced real-time adaptive feedback mechanisms, 3D printing can become more resilient against defects, improving both efficiency and print quality while minimizing material waste.

## 8 Conclusion and future directions

Defect detection in 3D printing is a critical area of research, driven by the increasing adoption of additive manufacturing technologies in high-stakes industries such as aerospace, healthcare, and automotive. While 3D printing offers significant advantages in terms of flexibility and design complexity, it is also prone to defects that can compromise the structural integrity, surface quality, and dimensional accuracy of the final product. Traditional post-production inspection methods are often insufficient, prompting the need for real-time monitoring systems that can detect and correct defects during the printing process.

The review highlights the evolution from classical to modern, deep learning–based approaches for defect detection. Classical methods rely on manually designed algorithms and predefined feature extraction techniques, which, while effective in certain cases, struggle to manage the complexity and high dimensionality of modern 3D printing processes. In contrast, deep learning models, particularly Convolutional Neural Networks (CNNs), offer significant improvements by automatically learning features and enabling more accurate, real-time detection of defects.

Additionally, the review compares full-reference and no-reference methods for defect detection. Full-reference methods provide high accuracy by comparing the printed part to an ideal reference model, while no-reference methods are more flexible, detecting visual or structural anomalies without the need for predefined models. Both approaches have their advantages, with full-reference methods excelling in precision environments and no-reference methods offering adaptability and ease of use.

As real-time defect detection technologies continue to advance, the integration of machine vision and deep learning promises to enhance the reliability, efficiency, and sustainability of 3D printing. Future trends point toward the development of more autonomous, closed-loop systems that adjust printing parameters dynamically, minimizing defects and material waste while ensuring the quality of printed components.

### 8.1 Practical applications

The application of defect detection techniques in 3D printing extends across multiple industries, including aerospace, healthcare, automotive, and consumer goods manufacturing. By integrating advanced defect detection systems, manufacturers can significantly enhance production quality, minimize material waste, and reduce costly post-production inspections. For instance, real-time monitoring systems in biomedical 3D printing can ensure the integrity of patient-specific implants, while in aerospace, defect detection prevents structural weaknesses in critical components.

### 8.2 Future directions

Further advancements in defect detection can be achieved through the following directions:

- Integration of edge computing: enhancing real-time decision-making by processing defect detection data locally rather than relying on cloud-based computation.
- Self-learning AI models: implementing adaptive machine learning techniques that improve detection accuracy over time by learning from newly identified defect patterns.
- Multi-sensor fusion systems: combining optical, thermal, and acoustic sensors to provide a more holistic approach to defect detection.
- Automated correction mechanisms: developing feedback-controlled printing adjustments to instantly rectify detected defects during the printing process.

These innovations will further advance the reliability and efficiency of 3D printing, making defect-free production more attainable and sustainable.

**Funding** This study received no specific funding from public, commercial, or non-profit sectors.

**Data Availability** All data used and cited in this review are available in the referenced sources.

## Declarations

**Ethics approval and consent to participate** No human participants or personal data involved.

**Consent for publication** No individual participant data requiring consent.

**Conflict of interest** The authors declare no competing interests.

## References

1. Oleff A, Küster B, Overmeyer L (2024) Determination of quality classes for material extrusion additive manufacturing using image processing. The International Journal of Advanced Manufacturing Technology 132:1585–1598
2. C. K. Chua and F. L. Kah. Printing and additive manufacturing: principles and applications of rapid prototyping, 3rd ed. World Scientific Publishing Company, 2016.
3. Oleff A, Küster B, Stonis M, Overmeyer L (2021) Process monitoring for material extrusion additive manufacturing: a state-of-the-art review. Progress in Additive Manufacturing 6:705–730
4. A. L. Petsiuka and J. M. Pearce. Open source computer vision-based layer-wise 3D printing analysis. Additive Manufacturing, vol. 36, 2020.
5. A. L. Petsiuka and J. M. Pearcea. Towards smart monitored AM: open source in-situ layer-wise 3D printing image anomaly detection using histograms of oriented gradients and a physics-based rendering engine. Additive Manufacturing, vol. 52, 2022.
6. G. D. Goh, N. M. Bin Hamzah and W. Y. Yeong. Anomaly detection in fused filament fabrication using machine learning. 3D printing and additive manufacturing, vol. 10, no. 3, 2023.
7. Z. Jin, Z. Zhang, X. Shao and G. X. Gu. Monitoring anomalies in 3D bioprinting with deep neural networks. ACS Biomaterials Science & Engineering, vol. 9, no. z, 2021.
8. M. Forte, M. Eisenhour, R. M. Malkowski, P. Radhakrishnan and D. C. Brown. Detecting defects in low-cost 3D printing. In ASME 2022 International Mechanical Engineering Congress and Exposition, Ohio, 2022.
9. Straub J (2015) Initial work on the characterization of additive manufacturing (3D printing) using software image analysis. Machines 3:55–71
10. D. B. Patil, A. Nigam and S. Mohapatr. An image processing approach to measure features and identify the defects in the laser additive manufactured components. In 4th International Conference on Recent Trends in Computer Science and Technology (ICRTCST-2021), 2021.
11. Bowoto OK, Oladapo BI, Zahed SA, Omigbodun FT, Emenuvwe OP (2020) Analytical modelling of in situ layer-wise defect detection in 3D-printed parts: additive manufacturing. The International Journal of Advanced Manufacturing Technology 111:2311–2321
12. Holzmond O, Li X (2017) In situ real time defect detection of 3D printed parts. Addit Manuf 17:135–142
13. Y. Fu, A. Downey, L. Yuan, A. Pratt and Y. Balogun. In situ monitoring for fused filament fabrication process: a review. Additive Manufacturing, vol. 38, 2021.
14. Caggiano A, Zhang J, Alfieri V, Caiazzo F, Gao R, Teti R (2019) Machine learning-based image processing for on-line defect recognition in additive manufacturing. CIRP Ann Manuf Technol 68:451–454
15. M. Muktadir and S. Yi. Machine vision-based detection of surface defects of 3D-printed objects. In ASEE Annual Conference, 2021.

16. J. Yan, S. Bai, Y. Li, X. Yu and C. Cai. A wire drawing defect detection approach for FDM 3D printing based on machine vision technology. In 5th International Conference on Artificial Intelligence and Computer Applications (ICAICA), 2023.
17. Zhang H, Zong Z, Yao Y, Hu Q, Aburaia M, Lammer H (2023) Multi-axis 3D printing defect detecting by machine vision with convolutional neural networks. Exp Tech 47:619–631
18. Wang W, Wang P, Zhang H, Chen X, Wang G, Lu Y, Chen M (2024) A real-time defect detection strategy for additive manufacturing processes based on deep learning and machine vision technologies. Micromachines 15(28):1–14
19. Zhou J, Li H, Lu L, Cheng Y (2024) Machine vision-based surface defect detection study for ceramic 3D printing. Machines 12(166):1–15
20. H. Shen, W. Du, W. Sun, Y. Xu and J. Fu. Visual detection of surface defects based on self-feature comparison in robot 3-D printing. Applied Science, vol. 10, no. 235, pp. -11, 2020.
21. Liu X, Li Y, Guo Y, Zhou L (2023) Printing defect detection based on scale-adaptive template matching and image alignment. Sensors 23(9):1–14
22. Kim RG, Abisado M, Villaverde J, Sampedro GA (2023) A survey of image-based fault monitoring in additive manufacturing: recent developments and future directions. Sensors 23(17):6821–6850
23. M. Wu, V. V. Phoha, Y. B. Moon and A. K. Belman. Detecting malicious defects in 3D printing process using machine learning and image classification. In ASME 2016 International Mechanical Engineering Congress and Exposition, Arizona, 2016.
24. A. I. Sadaf, H. Ahmed, M. A. Iqbal Khan and H. Sezer. Development of real-time defect detection techniques using infrared thermography in the fused filament fabrication process. In ASME 2023 International Mechanical Engineering Congress and Exposition, New Orleans, 2023.
25. E. C. de Santana, W. F. de Silva, M. G. Lima, G. R. Pereira and D. B. Riffe. Three-dimensional printed subsurface defect detection by active themography data-processing algorithm. 3D PRINTING AND ADDITIVE MANUFACTURING, vol. 10, no. 3, 2023.
26. Y. AbouelNour and N. Gupta. Assisted defect detection by in-process monitoring of additive manufacturing using optical imaging and infrared thermography. Additive Manufacturing, vol. 67, no. 5, 2023.
27. R. C. Gonzalez. Digital image processing. Pearson Education, 2009.
28. Ren Z, Fang F, Yan N, Wu Y (2021) State of the art in defect detection based on machine vision. International Journal of Precision Engineering and Manufacturing-Green Technology 9:661–691
29. R. Duda, P. Hart and D. Stork. Pattern classification, 2nd ed. John Wiley & Sons, 2001.
30. Bishop CM (2006) Pattern recognition and machine learning. Springer, New York, NY
31. LeCun Y, Bengio Y (2015) Deep learning. Nature 521(7553):436–444
32. Krizhevsky A, Sutskever I, Hinto GE (2017) ImageNet classification with deep convolutional neural networks. Commun ACM 60(6):84–90
33. Cheng Y, Jafari MA (2008) Vision-based online process control in manufacturing applications. IEEE TRANSACTIONS ON AUTOMATION SCIENCE AND ENGINEERING 5(1):140–153
34. S. Hurd, C. Camp and J. White. Quality assurance in additive manufacturing through mobile computing. In Mobile Computing, Applications, and Services (MobiCASE 2015), 2015.
35. A. Ceruti, A. Liverani and T. Bombardi. Augmented vision and interactive monitoring in 3D printing process. International Journal on Interactive Design and Manufacturing (IJIDeM), vol. 11, no. 2, 2016.
36. A. Johnson, H. Zarezadeh, X. Han, R. Bibb and R. Harris. Establishing in-process inspection requirements for material extrusion additive manufacturing. In Fraunhofer Direct Digital Manufacturing Conference, 2016.
37. Nuchitprasitchai S, Roggemann M, Pearce JM (2017) Factors effecting real-time optical monitoring of fused filament 3D printing. Progress in Additive Manufacturing 2:133–149
38. J. Straub. An approach to detecting deliberately introduced defects and microdefects in 3D printed objects. In Pattern Recognition and Tracking XXVIII, 2017.
39. R. A. Lyngby, J. Wilm, E. R. Eiríksson, J. B. Nielsen, J. N. Jensen and H. Aanæs. In-line 3D print failure detection using computer vision. In euspen and ASPE Special Interest Group Meeting: Additive Manufacturing: Dimensional Accuracy and Surface Finish from Additive Manufacturing, 2017.
40. Delli U, Chang S (2018) Automated process monitoring in 3D printing using supervised machine learning. Procedia Manufacturing 26:865–870
41. Malik A, Lhachemi H, Ploennigs J, Ba A, Shorten R (2019) An application of 3D model reconstruction and augmented reality for real-time monitoring of additive manufacturing. Procedia CIRP 18:346–351
42. F. Wasserfall, D. Ahlers and N. Hendrich. Optical in-situ verification of 3D-printed electronic circuits. In IEEE 15th International Conference on Automation Science and Engineering (CASE), 2019.
43. X. Xu, R. Wang, Q. Cao and C. Feng. Towards 3D perception and closed-loop control for 3D construction printing. In 37th ISARC, Kitakyushu, 2020.
44. C. Kopsacheilis, P. Charalampous, I. Kostavelis and D. Tzovaras. In situ visual quality control in 3D printing. In Proceedings of the 15th International Joint Conference on Computer Vision, Imaging and Computer Graphics Theory and Applications, 2020.
45. S. Rahmani Dabbagh, O. Ozcan and S. Tasoglu. Machine learning-enabled optimization of extrusion-based 3D printing. Methods, vol. 206, pp. 27–40, 2022.
46. R. Rill-García, E. Dokladalova, P. Dokládal, . J.-F. Caron, R. Mesnil, P. Margerit and M. Charrier. Inline monitoring of 3D concrete printing using computer vision. Additive Manufacturing, vol. 60, no. Part A, 2022.
47. Zhao X, Li Q, Xiao M, He Z (2023) Defect detection of 3D printing surface based on geometric local domain features. The International Journal of Advanced Manufacturing Technology 125:183–194
48. Bindera L, Racklb S, Scholza M, Hartmannb M (2023) Linking thermal images with 3D models for FFF printing. Procedia Computer Science 217:1168–1177
49. F. Baumann and D. Roller. Vision based error detection for 3D printing processes. In Proceedings of the MATEC Web of Conferences. EDP Sciences, Amsterdam, 2016.
50. J. Fastowicz and K. Okarma. Texture based quality assessment of 3D prints for different lighting conditions. In Computer Vision and Graphics, 2016.
51. W. Yi, H. Ketai, Z. Xiaomin and D. Wenying. Machine vision based statistical process control in fused deposition modeling. In 12th IEEE Conference on Industrial Electronics and Applications (ICIEA), 2017.
52. K. Okarma, J. Fastowicz and M. Tecław . Application of structural similarity based metrics for quality assessment of 3D prints. In Computer Vision and Graphics. ICCVG 2016, 2016.
53. K. Okarma and J. Fastowicz. Color independent quality assessment of 3D printed surfaces based on image entropy. In 10th International Conference on Computer Recognition Systems CORES 2017, 2017.

54. H. Shen, W. Sun and J. Fu. Multi-view online vision detection based on robot fused deposit modeling 3D printing technology. Rapid Prototyping Journal, vol. 25, no. 2, 2018.
55. Kazemian A, Yuanc X, Davtalaba O, Khoshnevis B (2019) Computer vision for real-time extrusion quality monitoring and control in robotic construction. Autom Constr 101:92–98
56. Okarma K, Fastowicz J (2019) Adaptation of full-reference image quality assessment methods for automatic visual evaluation of the surface quality of 3D prints. ELEKTRONIKA IR ELEKTROTECHNIKA 25(5):57–62
57. Fastowicz J, Grudzinski M, Tecław M, Okarma K (2019) Objective 3D printed surface quality assessment based on entropy of depth maps. Entropy 21(97):1–13
58. K. Okarma and J. Fastowicz. Computer vision methods for non-destructive quality assessment in additive manufacturing. In Progress in Computer Recognition Systems. CORES 2019, 2019.
59. Fastowicz J, Okarma K (2019) Quality assessment of photographed 3D printed flat surfaces using Hough transform and histogram equalization. J Univ Comput Sci 25(6):701–717
60. K. Okarma and J. Fastowicz. Improved quality assessment of colour surfaces for additive manufacturing based on image entropy. Pattern Analysis and Applications, pp. 1035–1047, 2020.
61. Liu C, Law ACC, Roberson D, Kong Z (2019) Image analysis-based closed loop quality control for additive manufacturing with fused filament fabrication. J Manuf Syst 51:75–86
62. G. Mohr, S. J. Altenburg, A. Ulbricht, P. Heinrich, D. Baum, C. Maierhofer and K. Hilgenberg. In-situ defect detection in laser powder bed fusion by using thermography and optical tomography—comparison to computed tomography. Methods, vol. 10, 2020.
63. Mazzarisi M, Angelastro A, Latte M, Colucci T, Palano F, Campanelli SL (2023) Thermal monitoring of laser metal deposition strategies using infrared thermography. J Manuf Process 85(6):594–611
64. Höfflin D, Sauer C, Schiffler A, Versch A, Hartmann J (2024) Active thermography for in-situ defect detection in laser powder bed fusion of metal. J Manuf Process 131:1758–1769
65. Montinaro N, Cerniglia D, Pitarresi G (2017) A numerical and experimental study through laser thermography for defect detection on metal additive manufactured parts. Fracture and Structural Integrity 12(43):231–240
66. J. Sun, K. Yao, J. An, L. Jing, K. Huang and D. Huang. Machine learning and 3D bioprinting. International Journal of Bioprinting, vol. 9, no. 4, 2023.
67. Y. Niu, E. Chadwick, A. W. Ma and Q. Yang. Semi-Siamese network for robust change detection across different domains with applications to 3D printing. arXiv, 2023.
68. O. Charia, H. Ranjani, I. Ferrer Real, M. Domingo-Espin and N. Gracias. Real-time stringing detection for additive manufacturing. Journal of Manufacturing and Materials Processing, vol. 9, no. 3, 2025.
69. Jin Z, Zhang Z, Gu GX (2019) Autonomous in-situ correction of fused deposition modeling printers using computer vision and deep learning. Manufacturing Letters 22:11–15
70. N. Razaviaraba, S. Sharifib and Y. M. Banadaki. Smart additive manufacturing empowered by a closed-loop machine learning algorithm. Proceedings of the SPIE, vol. 10969, 2019.
71. Y. Banadaki, N. Razaviarab, H. Fekrmandi and S. Sharifi. Toward enabling a reliable quality monitoring system for additive manufacturing process using deep convolutional neural networks. In Arxiv, 2020.
72. Garfo S, Muktadir M, Yi S (2020) Defect detection on 3D print products and in concrete structures using image processing and convolution neural network. Journal of Mechatronics and Robotics 4(1):74–84
73. Baumgartl H, Tomas J, Buettner R, Merkel M (2020) A deep learning-based model for defect detection in laser-powder bed fusion using in-situ thermographic monitoring. Progress in Additive Manufacturing 5:277–285
74. K. Paraskevoudis, P. Karayannis and E. p. Koumoulos. Real-time 3D printing remote defect detection (stringing) with computer vision and artificial intelligence. Processes, vol. 8, 2020.
75. M. Farhan Khan, A. Alam, M. A. Siddiqui, M. S. Alam, Y. Rafat, N. Salik and I. Al-Saidan. Real-time defect detection in 3D printing using machine learning. Materials Today: Proceedings, vol. 42, pp. 521–528, 2021.
76. Brion DA, Shen M, Pattinson SW (2022) Automated recognition and correction of warp deformation in extrusion additive manufacturing. Addit Manuf 56:1–10
77. Brion DAJ, Pattinson SW (2022) Generalisable 3D printing error detection and correction via multi-head neural networks. Nat Commun 13:1–14
78. Nguyen PD, Nguyen TQ, Tao QB, Vogel F, Nguyen-Xuan H (2022) A data-driven machine learning approach for the 3D printing process optimisation. Virtual and Physical Prototyping 17(4):768–786
79. M. Cao, L. Fu, K. Zhou and F. Ai. Improved 3D printing extrusion defect detection method based on Yolo-V8. SSRN, 2024. [Online]. Available: https://ssrn.com/abstract=4800007.
80. W. Hu, C. Chen, S. Su, J. Zhang and A. Zhu. Real-time defect detection for FFF 3D printing using lightweight model deployment. The International Journal of Advanced Manufacturing Technology, vol. 134, 2024.
81. B. Aksoy and K. Ozsoy. Deep learning-based classification of 3D printing defects. In International Scientific Research and Innovation Congress, Venedik, 2024.
82. M. Singh, P. Sharma, S. K. Sharma and J. Singh. A novel real-time quality control system for 3D printing: a deep learning approach using data efficient image transformers. Expert Systems with Applications, vol. 273, 2025.
83. B. Szymanik, G. Psuj, M. Hashemi and P. Lopato. Detection and identification of defects in 3D-printed dielectric structures via thermographic inspection and deep neural networks. Materials, vol. 14, 2021.
84. G. Bilowo and B. Hardjono. 3D print orientation optimization and comparative analysis of NSGA-II versus NSGA-II with Q-learning. International Journal on Smart Sensing and Intelligent Systems, vol. 18, no. 1, 2025.
85. S. Dharmadhikari, N. Menon and A. Basak. A reinforcement learning approach for process parameter optimization in additive manufacturing. arXiv, 2022.
86. X. Li and S. Pattinson. An efficient and uncertainty-aware reinforcement learning framework for quality assurance in extrusion additive manufacturing. arXiv, 2025.
87. A. Alghamdi. Enhancing 3D printing workflows through multi-objective optimization and reinforcement learning techniques. Engineering, technology & applied science research, vol. 15, no. 2, 2025.